PHYSICAL REVIEW C **87**, 064301 (2013)

γ-ray spectroscopy of the $A = 23$, $T = 1/2$ nuclei ^{23}Na and ^{23}Mg: High-spin states, mirror symmetry, and applications to nuclear astrophysical reaction rates

D. G. Jenkins,[1,*] M. Bouhelal,[2] S. Courtin,[3] M. Freer,[4] B. R. Fulton,[1] F. Haas,[3] R. V. F. Janssens,[5] T. L. Khoo,[5] C. J. Lister,[5,†] E. F. Moore,[5] W. A. Richter,[6] B. Truett,[5] and A. H. Wuosmaa[5,‡]

[1]*Department of Physics, University of York, York YO10 5DD, United Kingdom*
[2]*Laboratoire de Physique Appliquée et Théorique, Université de Tébessa, Tébessa, Algeria*
[3]*IPHC, Université de Strasbourg, CNRS-IN2P3, Strasbourg, France*
[4]*School of Physics and Astronomy, University of Birmingham, Birmingham B15 2TT, United Kingdom*
[5]*Physics Division, Argonne National Laboratory, Argonne, Illinois 60439, USA*
[6]*iThemba Labs, P.O. Box 722, Somerset West 7129, South Africa and Department of Physics, University of the Western Cape, Private Bag X17, Bellville 7535, South Africa*

(Received 27 March 2013; published 4 June 2013)

Background: Obtaining reaction rates for nuclear astrophysics applications is often limited by the availability of radioactive beams. Indirect techniques to establish reaction rates often rely heavily on the properties of excited states inferred from mirror symmetry arguments. Mirror energy differences can depend sensitively on nuclear structure effects.

Purpose: The present work sets out to establish a detailed comparison of mirror symmetry in the $A = 23$, $T = 1/2$ mirror nuclei ^{23}Na and ^{23}Mg both to high spin, and high excitation energy, including beyond the proton threshold. These data can be used to benchmark state-of-the-art shell-model calculations of these nuclei.

Methods: Excited states in ^{23}Na and ^{23}Mg were populated using the ^{12}C(^{12}C,p) and ^{12}C(^{12}C,n) reactions at beam energies of 16 and 22 MeV, and their resulting γ decay was measured with Gammasphere.

Results: Level schemes for ^{23}Na and ^{23}Mg have been considerably extended; highly excited structures have been found in ^{23}Na, as well as their counterparts in ^{23}Mg for previously known rotational structures in ^{23}Na. Mirror symmetry has been investigated up to an excitation energy of 8 MeV and spin-parity of $13/2^+$. Excited states in the region above the proton threshold have been studied in both nuclei.

Conclusions: A detailed exploration of mirror symmetry has been performed which heavily constrains expectations as to how mirror energy differences should evolve for different structures. Agreement with shell-model calculations provides confidence in using such estimations where real data are absent.

DOI: 10.1103/PhysRevC.87.064301 PACS number(s): 27.30.+t, 21.10.Tg, 21.10.Re, 23.20.Lv

I. INTRODUCTION

Mirror nuclei, which are equivalent under change of isospin, reveal striking examples of the relative charge independence of the nuclear force. A key indicator of divergences from strict mirror symmetry, due to charge-dependent effects, is found in the mirror energy difference (MED), defined as the energy difference between analog states in the two partner nuclei, where the large mass difference between the mirror nuclei is neglected. MEDs have been shown to be sensitive to nuclear structure effects such as particle alignments and termination of the valence space [1,2]. Indeed, this behavior has been studied in detail in the fp shell, for example, for mirror pairs such as ^{47}V and ^{47}Cr [3] and ^{49}Cr and ^{49}Mn [4]. In general, knowledge about mirror symmetry in lighter nuclei is less well developed. This, perhaps, reflects less on the relative difficulty of studying such nuclei and more on the fact that the nuclear structure involved increases in complexity when multiple shells are occupied. Nevertheless, recent explorations of mirror symmetry in the sd-fp shell include the $A = 35$ [5] and $A = 31$ mirror pairs [6]. Large isolated values for the MED have been observed for certain states which have been attributed to the electromagnetic spin-orbit interaction. In both these mirror pairs, unusual behavior has been seen in terms of differing strengths of $E1$ transitions which has been linked to the effects of isospin mixing [7].

A separate motivation for studying mirror symmetry in light nuclei is related to nuclear astrophysics. In particular, such studies can provide complementary data for obtaining reaction rates for proton capture reactions which are important in the rp process occurring in astrophysical scenarios such as novas [8,9]. In the case of a prototypical proton capture reaction of the form $X(p,\gamma)Y$, the progenitor nucleus X is often a short-lived radioactive species which is impossible to produce as a target material. This same nucleus is often equally difficult to produce as an accelerated beam in sufficient intensity to perform the proton capture reaction directly in inverse kinematics. In some special cases, the latter has, nevertheless, been achieved; for example, a direct measurement of the ^{21}Na(p,γ) reaction in inverse kinematics using a radioactive ^{21}Na beam was carried out at the ISAC facility at TRIUMF [10]. Where direct

*david.jenkins@york.ac.uk
†Present address: Department of Physics, University of Massachusetts, Lowell, MA 01854.
‡Present address: Department of Physics, Western Michigan University, Kalamazoo, MI 49008.

measurements are not possible, an alternative is to collate detailed spectroscopic information on states in the Gamow window in the fused nucleus, Y, which can help in making indirect assessments of the proton capture rate. There are a wide variety of techniques which can be used to build up this picture ranging from beta-decay spectroscopy to transfer reactions. Transfer reactions such as (^{3}He,t) can be used simply to hunt for levels in a nonselective manner, while reactions such as (^{3}He,d) can be used as surrogates to (p,γ) reactions and can deliver valuable information on proton spectroscopic factors for states of interest in the Gamow window.

A technique developed over the last decade consists of using γ-ray spectroscopy to infer properties of states of interest in the Gamow window using high-resolution arrays of high-purity germanium detectors such as Gammasphere [11]. This technique can deliver the excitation energies of states with sub-keV accuracy, which is impossible from transfer measurements, and which essentially removes the uncertainty due to resonance energies. Moreover, the spin and parity of such states can be inferred on the basis of γ-ray angular distributions but also, importantly in the context of the present discussion, from comparisons of decay branchings of analog states in the mirror system. This approach has now been applied to a large number of cases with astrophysical relevance. For example, reaction rates were obtained for the ^{22}Na(p,γ)^{23}Mg reaction using updated information on the relevant states in ^{23}Mg obtained from the ^{12}C(^{12}C,n) reaction [12] making heavy use of comparisons to mirror states in ^{23}Na. In a separate study, Seweryniak *et al.* studied proton-unbound states in ^{22}Mg produced in the ^{12}C(^{12}C,2n) reaction [13]. This work is highly complementary to direct ^{21}Na(p,γ)^{22}Mg studies performed at TRIUMF [10], since it was possible by means of mirror symmetry arguments to show that the direct measurements had, indeed, exhausted all the relevant resonances in this reaction. Moreover, this work showed that the adopted energy of the 5714-keV level was in error and this suggested a revision of the ^{22}Mg mass, which is relevant to standard model tests of the conserved vector current hypothesis [13]. Since these early examples, a series of experiments have been carried out with very similar methodology using the Gammasphere array. These have provided important information, for example, on the ^{25}Al(p,γ)^{26}Si reaction by exploiting mirror symmetry in ^{26}Si and ^{26}Mg [14]; the ^{30}P(p,γ) reaction from consideration of the $A = 31$ mirror nuclei, ^{31}S and ^{31}P [15]; ^{23}Mg(M,γ)^{24}Al [16]; and ^{26}Al(p,γ)^{27}Si [17]. Typically, each of these publications has presented only a narrow subset of the levels in the mirror comparison. In contrast, Lotay *et al.* have recently presented a detailed comparison of mirror symmetry in the $A = 27, T = 1/2$ mirror pair [18]. This in-depth analysis is instructive since it starts to generate a reliable empirical prescription for the location of mirror states, which is important for cases where experimental information is limited and where, in the past, global mirror energy shifts of 200 keV have been suggested [19].

Despite the long-standing interest and study of the sd-shell nuclei, new features are still emerging, in particular with regard to highly excited and very-high-spin states (where high spin in this mass region can mean $J \sim 8\,\hbar$). Moreover, there is a long-standing search for highly deformed configurations such as superdeformed bands which may be present in, for example, ^{28}Si [20] and ^{32}S. In terms of high-spin states, the classic example is ^{24}Mg, which has a notably complex yrast line with three close-lying 8^+ states, of which the lowest is not a member of the ground-state rotational band, but rather corresponds to a spherical configuration. Notwithstanding the intense study of ^{24}Mg over the years, a sophisticated combination of α-γ coincidences was required to unambiguously determine the location of the first 10^+ state at 19.2 MeV in ^{24}Mg [21], and to observe a very weak 5927-keV γ ray connecting the 10^+ level to the second 8^+ state, which is suggested to be a member of the ground-state rotational band.

Just as it has proved difficult to locate high-spin states in the sd-shell nuclei, it has also not been straightforward to fully realize shell-model calculations by locating the complete set of sd orbitals. For example, the [202]3/2 deformed rotational band in ^{25}Al and ^{25}Mg was identified for the first time over 50 years since its first prediction [22]. Further work on the sd shell has seen efforts towards complete spectroscopy of the odd-odd nuclei ^{26}Al and ^{30}P [23]. A complete identification of the spins, parities, and isospin quantum numbers of low-lying $T = 0$ and $T = 1$ states is only really possible for sd-shell nuclei, and the results of these compilations may be used to draw important conclusions about isospin symmetry breaking [24].

Excited states in sd-shell nuclei have mostly been studied through reaction studies or beta-decay measurements. When germanium detectors have been employed, this has generally been on an individual basis and not in large arrays (with the possible exception of the high-spin studies in ^{24}Mg mentioned above). The focus of attention with large 4π arrays of suppressed germanium detectors has been the rotational properties of medium-heavy mass nuclei, and sd-shell nuclei have been largely bypassed. This is unfortunate since, as the present work will demonstrate, there is much new and important information on the structure of sd-shell nuclei to be extracted with γ-ray spectroscopy techniques. For example, producing sd-shell nuclei in fusion evaporation reactions and studying their decay with a large array of germanium detectors may allow high-spin states, especially those which do not lie on the yrast sequence, to be studied in detail. In particular, their decay branchings can be observed and their lifetimes may be extracted; both of which can put strong constraints on sd-shell-model calculations. Indeed, it may also be possible to study the influence of intruder configurations.

In the present work, extensive information is presented on the excited states of the mirror nuclei ^{23}Na and ^{23}Mg originating from a study with the Gammasphere array. A small subset of the information given here was presented in an earlier publication in Physical Review Letters [12], which focused exclusively on proton-unbound levels in ^{23}Mg relevant to the the ^{22}Na(p,γ) reaction. Here, the data appears in its full context. A large number of excited states are identified for the first time in both nuclei, and lifetimes are measured in some cases allowing a detailed comparison with shell-model calculations for both positive- and negative-parity states. Information on the newly identified excited states in both ^{23}Na and ^{23}Mg, and their decays allow MEDs to be explored for both yrast and non-yrast states. These may again be compared with shell-model calculations, providing an important input in

predicting the location of high-lying states relevant to rates for the ^{22}Na(p,γ) and ^{22}Ne(p,γ) reactions.

II. PREVIOUS STUDIES OF ^{23}Na AND ^{23}Mg

In the past, excited states in ^{23}Na and ^{23}Mg have been extensively studied with a broad range of nuclear spectroscopic techniques. This previous work can be broadly divided into two categories: nuclear structure studies and those directed specifically at studying proton-unbound states, with the motivation of extracting a rate for the respective proton capture reaction.

A. Nuclear structure studies

In order to investigate high-spin states it is necessary to employ heavy-ion fusion-evaporation reactions such as ^{12}C(^{12}C,$p\gamma$) and ^{12}C(^{12}C,$n\gamma$) [25–28]. In addition to the ^{12}C + ^{12}C reaction, studies of high-spin states in ^{23}Na have also been performed with reactions of varying selectivity such as ^{19}F(^{6}Li,d)^{23}Na [29] and ^{12}C(^{15}N,α)^{23}Na [30,31]. Indeed, these have been employed in conjunction with proton-γ and neutron-γ coincidence measurements to tentatively assign states as high as $J^{\pi} = 21/2^{+}$ in the ground-state bands of ^{23}Mg [25] and ^{23}Na [31]. In recent work, limited to low spin states, the mirror symmetry of ^{23}Na and ^{23}Mg was investigated by studying $M1$ and Gamow-Teller transitions [32].

B. Nuclear astrophysics studies

There are a number of papers reporting revised estimates for the ^{22}Na(p,γ) and ^{22}Ne(p,γ) reaction rates. The direct approach is problematic since it involves the use of either a strongly radioactive target in the former case, or in the latter a gas or implanted target. Seuthe *et al.* found a series of resonances in the ^{22}Na(p,γ) reaction for $E_p = 0.17$ to 1.29 MeV [33], while Stegmüller *et al.* repeated this study for $E_p = 0.20$ to 0.63 MeV and found a new resonance at $E_p = 213$ keV [34]. Additional information relevant to the ^{22}Na(p,γ) reaction can be obtained from transfer reactions such as ^{24}Mg(p, d) [35] and ^{22}Na(^{3}He,d) [36]. A further means of obtaining indirect information on unbound states is via beta decay [37–39].

In an earlier publication based on the data set presented here, Jenkins *et al.* [12] presented new data on proton-unbound states in ^{23}Mg and highlighted the possible role of an additional resonance at $E_p = 198$ keV. In the present work, these data are discussed in more detail and in their full context. Very recently, Sallaska *et al.* carried out a new direct study of the ^{22}Na(p,γ) reaction using an implanted target [40]. This measurement has now very strongly reduced the remaining uncertainties for this particular reaction, and largely supersedes the need for indirect measurements in this particular case.

In terms of the ^{22}Ne(p,γ) reaction, efforts have been made to study the direct capture contribution to the (p,γ) reaction by Görres *et al.* with the help of a ^{22}Ne gas target [41]. A reevaluation of the ^{22}Ne(p,γ) reaction using data extracted from a (^{3}He,d) spectroscopic study was presented by Hale *et al.* [42] using a ^{22}Ne-doped ^{nat}C foil.

III. METHODOLOGY

In order to study simultaneously the γ decay of both high-spin and proton-unbound states in the $A = 23$, $T = 1/2$ mirror pair, the Gammasphere array of 100 high-purity germanium (HPGe) detectors was employed, in a somewhat unorthodox fashion. This array was principally designed to detect high-multiplicity cascades of transitions associated with rotational structures in nuclei; the paradigm of such work being superdeformed bands [43], where the energy of the transitions in the rotational bands is usually in the approximate range 200–2000 keV, while the γ-ray multiplicity might be as high as 30 since levels of very high angular momentum, up to 70$\hbar$, are populated [43]. When rotational structures are investigated in heavy nuclei, an array such as Gammasphere is generally operated in a high-fold coincidence mode requiring four or even five γ rays to be cleanly detected, which greatly reduces the dead time in the readout. By contrast, in light nuclei, such as ^{23}Na and ^{23}Mg, a $J = 13/2$ state might correctly be labeled as "high spin", and the associated γ-ray multiplicity is correspondingly low, with a mean multiplicity of around 3. Due to the low level density and phase space considerations, which favor out-of-band rather than in-band transitions for excited rotational bands, high-energy γ rays are expected with energies up to 10 MeV. The energy and fold distribution of the γ rays involved in the decay of such light nuclei, therefore, pose a strong challenge to the design of the array. Despite the difficulties that might be expected, the present work clearly demonstrates that Gammasphere, which is more usually employed in the detection of γ rays of around 1–2 MeV, is equally capable of resolving γ rays with energies in excess of 10 MeV, decaying from states as much as 4 MeV proton unbound. In such highly unbound regions, the γ branch is typically very small compared to the dominant particle decay. Nevertheless, this study proves that with a full 4π solid angle coverage and with modest high-energy efficiency, it is possible to carry out a detailed examination of these unbound states.

IV. EXPERIMENTAL DETAILS

Accelerated beams of ^{12}C from the ATLAS accelerator at Argonne National Laboratory at energies of 16 and 22 MeV were incident on an enriched 160 μg/cm^2 ^{12}C target. The resulting γ decay was detected by the Gammasphere array [11]. The only fusion-evaporation channels open at these energies were those involving one proton, one neutron, or one alpha emission leading to ^{23}Na, ^{23}Mg, and ^{20}Ne, respectively. Since the level scheme for the low-spin states in ^{23}Na was rather well known, and some information on transitions in ^{23}Mg was available, it was unnecessary to apply any specific identification of the recoiling nucleus or of emitted particles. The previously known level schemes for ^{23}Na and ^{23}Mg were verified and enlarged using standard γ-ray spectroscopy techniques using coincidence γ-γ matrices and γ-γ-γ cubes generated from the data taken at the two beam energies. The γ-γ-γ cube from the 16-MeV data had around 2×10^8 triples events, while that from the 22-MeV data contained around 3×10^9. The difference in entry distribution at the two energies was exploited to assist in placing γ rays and resolving doublets.

All spectroscopic data presented in the tables below originate from the 22-MeV data.

The unorthodox usage of Gammasphere implied that greater caution had to be applied in extracting both γ-ray energies and intensities; these issues are worthy of detailed comment. In obtaining accurate energies, it was necessary to correct the measured values for the nonlinearity of the electronics of the array as well as for the non-negligible recoil for high-energy γ rays emitted from a light nucleus. The nonlinearity was inferred from source data for 25 standard γ rays from the decay of ^{152}Eu and ^{56}Co. This linearity curve was extended to higher energies with data from inelastic scattering of 7.5-MeV protons on a ^{11}B target which produces γ rays up to 5 MeV as well as the 6.129-MeV line from the the excitation of ^{16}O contaminant in the boron target. This nonlinearity correction was then applied in the present experiment and comparisons were also made with the literature values for previously known transitions [44]. In addition, in cases where two coincident transitions were crossed over by a third one, the corrected energy sum was compared and found, in nearly all cases, to be in agreement within a margin of 1 keV and in most cases to within 0.5 keV.

Extracting intensities for the high-energy transitions in the present work is not straightforward since the empirical efficiency curve is derived from source data for which the highest data point is around 3.5 MeV (from a ^{56}Co source). The efficiency curve may be extrapolated to higher energies by taking into account the expected functional response of the detectors. The latter response for high-energy γ rays was modeled using the Monte Carlo simulation code MCNP. In order to assign the multipolarity of the observed transitions, matrices were generated of all γ rays against those detected at 90° as well as of all γ rays against those detected at 32° and 37°. The ratio of the intensities of transitions in these two matrices, when gating on the "all" axis, was extracted. This ratio was 0.9(1) for pure stretched-dipole transitions and 1.8(1) for pure stretched-quadrupole ones. In the present case, these are best represented by $E1$ and $E2$ transitions since the mixing with $M2$ and $M3$ multipolarities, respectively, would be expected to be small. The angular correlation ratios obtained in the present work, for well-known stretched $E1$ and $E2$ transitions in ^{23}Na are presented in Fig. 1.

In the case of $M1$ transitions, more extensive mixing with $E2$ multipolarity is to be expected. Thus, mixed transitions take on intermediate values of the angular correlation ratio, depending on the value of the $M1/E2$ mixing ratio. For unstretched $M1/E2$, $J^\pi \rightarrow J^\pi$ transitions, the angular correlation may have the same value as for stretched-$E2$ transitions. Despite these caveats, in many cases the angular correlation measurements can be used in conjunction with the observed branching in the decay of a state to several levels of previously known spin and parity, to effectively constrain the quantum numbers of newly observed levels. In cases where this is not possible, however, additional considerations related to the study of light nuclei must be taken into account. While, in general, for heavy nuclei, fusion-evaporation reactions favor the population of high-spin states and decay down the yrast line—the line connecting states of lowest energy for a given spin—this is not necessarily true for light nuclei. For example, population of a

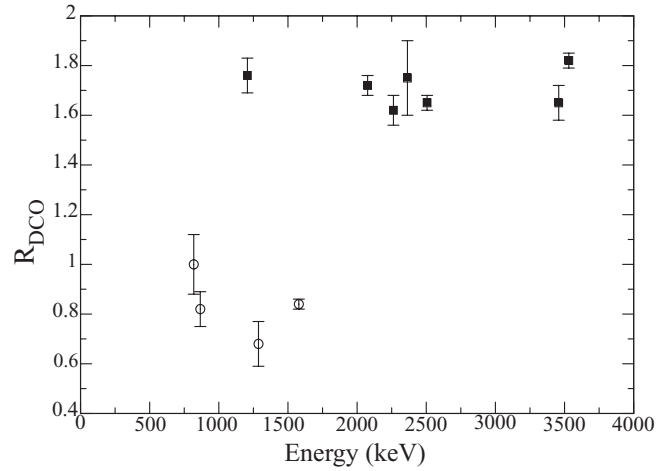

FIG. 1. Angular correlation ratios for γ rays of well established multipolarity in ^{23}Na. The open circles are known stretched-$E1$ transitions while the filled squares are stretched-$E2$ ones.

previously known $1/2^+$ state in ^{23}Na with an excitation energy close to 9 MeV was observed here. This excitation energy is above the proton separation energy of 8794 keV. In addition, the low level density in light nuclei implies that it is often possible to observe transitions which connect a state of lower to one with higher angular momentum. For this reason, for transitions where viable angular correlation information does not exist, all the possible spin values consistent with it decaying to a level with both lower or higher angular momentum have been quoted. In addition to considerations relating to angular correlations, mirror symmetry arguments were also used to support spin-parity assignments, particularly for states in the less well known nucleus ^{23}Mg. In this case, the criteria for the identification of mirror states were the closeness in level energy and the similarity in the branching of the decay to other levels. Individual mirror symmetry arguments are discussed in detail below.

For several of the high-lying states in both ^{23}Na and ^{23}Mg, it was also possible to deduce lifetimes using the fractional Doppler shift technique. The Doppler shift was extracted for γ rays emitted from states fed directly in the reaction, which is a safe assumption for unbound states, and may be verified in the γ-ray coincidence analysis. This condition is necessary to avoid complexities concerning feeding lifetimes. The experimental Doppler shift was determined by measuring the centroid of the γ ray of interest for each of the 17 rings of Gammasphere, which span the angular range 17° to 163° with respect to the beam axis. In order to produce clean spectra for this analysis, a coincidence requirement with transitions below the γ ray of interest was applied. The experimental Doppler shift was subsequently compared with the lifetime-dependent shift expected from a model of the slowing-down process in the carbon target. This model treated the kinematics of the two-body reaction of the type $A(a,b)B^*$ in order to deduce the recoil cone and, subsequently, correctly average the recoil velocity for the specific nucleus. The model treated the target as being composed of 500 slices, and a numerical integration was performed for various trial lifetimes. The fractional Doppler

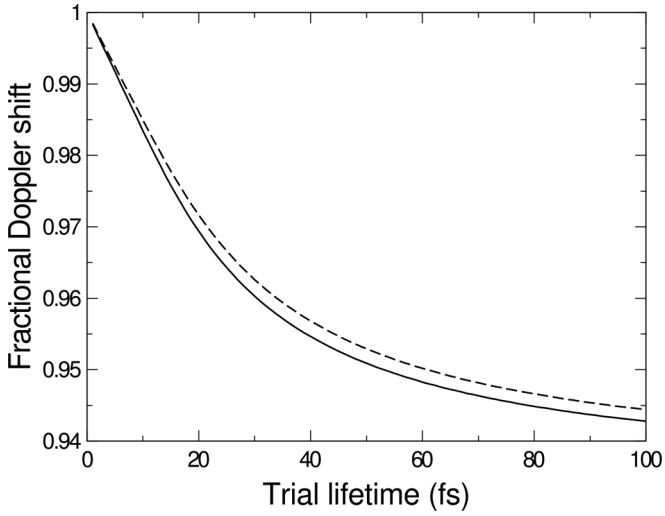

FIG. 2. Fractional Doppler shifts as a function of the trial lifetime calculated using the model described in the text. The solid curve is for ^{23}Mg residues, while the dashed curve is for ^{23}Na ones.

shift technique was found to be suitable for lifetimes in the 1–100 fs range (see Fig. 2) which is a range of values compatible with the expected lifetimes for high-lying states in the nuclei of interest.

V. RESULTS

A. Presentation of the data

Over 160 γ rays associated with the decay of excited states in ^{23}Na were observed in addition to a large number of new transitions in ^{23}Mg. In order to put the results from the present work in an easy-to-read format, it has been necessary to make certain decisions regarding their presentation. The full results of the spectroscopic analysis are presented in Tables I and II for ^{23}Na and ^{23}Mg, respectively. The tabulations include the energy and intensity of the observed γ rays, the angular correlation for those transitionss where it could be extracted, the suggested multipolarity and the assignment of the spin-parity of the deexciting state. Table III presents the results of the lifetime analysis for selected high-spin states in both nuclei. Example spectra derived from the γ-γ-γ coincidence analysis can be found in Figs. 3 and 4.

In order to simplify the discussion, a somewhat arbitrary separation of the level schemes into two parts was made, corresponding to states of presumed positive and negative parity, respectively. Furthermore, these level schemes only seek to represent the high-spin rotational states, meaning that a large number of levels are suppressed. The decision to separate positive and negative parity states also implies that many transitions which connect states of different parity are not shown in the level schemes, but these are discussed in the text where these are important to the spin-parity assignments of individual states.

B. Positive-parity rotational bands

Detailed spectroscopy of high-spin states in ^{23}Na was possible in the present work (see Fig. 5). The low-lying states of ^{23}Na were already well established. However, many of the higher-lying, high-spin states were observed in reaction studies [25,26,28] and their spin-parity assignment was uncertain. In the present work, the γ rays associated with the decay of these states were observed and, in many cases, their multipolarity was determined from angular correlation data. The spin-parity of high-spin states were firmly established as a result. The yrast cascade in ^{23}Na was delineated as far as the first $17/2^+$ state.

Due to the Q value for the ^{12}C(^{12}C,n) reaction, it was not possible to observe states above $\sim$8 MeV in ^{23}Mg. It was possible, however, to examine mirror symmetry for the ^{23}Na/^{23}Mg pair as high as the first two $J^\pi = 13/2^+$ states (see Fig. 6). For the near-yrast levels below the proton threshold, the agreement is good. This direct correspondence becomes more difficult to establish for states at higher excitation energy, and for those lying further from the yrast line. Specific examples are discussed below.

The shell model has long been employed to describe positive-parity states in sd-shell nuclei. In the present work, new shell-model calculations were carried out with a Hamiltonian derived by Ormand and Brown [45], which includes the USDB [46] effective interaction as the charge-independent part. The charge-dependent part has Coulomb and isospin nonconserving terms fitted to experimental data. This composite interaction is called USDB-cdpn in the NUSHELLX suite of codes [47]. The "cd" refers to charge-dependent, and "pn" indicates that the calculations are done in the proton-neutron formalism. Transition strengths are calculated with optimal effective charges and g factors, determined from fits to large numbers of magnetic and quadrupole moments, and from transition strengths [48]. A comparison of near-yrast positive-parity states in ^{23}Na with the present sd-shell-model calculations is given in Fig. 7. It can be seen that there is good agreement with theory in terms of excitation energy and decay branching for near-yrast states, in particular for the ground-state band. For some bands, the difference between the predicted excitation energy and experimental energy is larger; e.g., around 200 keV for the $K = 1/2^+$ band (see Fig. 8).

1. Location of the highest-spin positive-parity states in ^{23}Na

There is some disagreement in the literature over the spin-parity of the 9038- and 9802-keV levels in ^{23}Na. The state at 9038 keV has a well established spin-parity of $15/2^+$, while there is some debate over whether the level at 9802 keV has a spin-parity of $15/2^+$ or $17/2^+$. Kekelis *et al.* ruled out the possibility of a $J = 17/2$ assignment to either of these states [26,27], while Evers *et al.* [25], Green *et al.* [49], and Back *et al.* [50] favor a $17/2^+$ assignment to the 9802-keV state. These assignments were based on proton-γ correlations and lifetime measurements. The present work is in agreement with Kekelis *et al.* [27] since the angular correlation measurements suggest a $15/2^+$ assignment to the 9802-keV state, and this is supported by the observation of a prompt decay from this level to the well established $11/2^+$ level at 5533 keV [51]. A candidate for a third $15/2^+$ state was also identified at an

TABLE I. Spectroscopic information for ^{23}Na from the present work.

E_γ (keV)	I_γ (%)	R_{DCO}	M_λ	Assignment	E_i (keV)	E_f (keV)
170	1.3(3)			$5/2^- \rightarrow 3/2^-$	3848	3677
312	0.6(1)			$9/2^- \rightarrow 7/2^-$	6353	6041
440		0.95(1)	$M1/E2$	$5/2^+ \rightarrow 3/2^+$	440	0
591	3(1)			$3/2^+ \rightarrow 1/2^+$	2982	2391
627	352(2)	0.90(1)	$M1/E2$	$9/2^+ \rightarrow 7/2^+$	2703	2076
701	20(1)	0.90(2)	$M1/E2$	$13/2^+ \rightarrow 11/2^+$	6234	5533
819	4(1)	1.00(12)	$E1$	$9/2^- \rightarrow 11/2^+$	6353	5533
860	6(1)	0.91(10)	$M1$	$7/2^+ \rightarrow 5/2^+$	4775	3914
866	1.6(4)	0.82(7)	$E1$	$5/2^- \rightarrow 3/2^+$	3848	2982
932	0.8(2)			$5/2^+ \rightarrow 3/2^+$	3914	2982
984	3(1)			$9/2^- \rightarrow 7/2^+$	8822	7834
1033	5(1)	1.56(16)	J^π-J^π	$13/2^+ \rightarrow 13/2^+$	7267	5533
1037	2(1)	0.81(2)	$M1$	$3/2^- \rightarrow 1/2^-$	3677	2640
1070	6(1)	0.76(7)	$E1$	$(11/2^+) \rightarrow 13/2^-$	11422	10352
1087	2(1)			$(3/2, 11/2) \rightarrow 7/2^-$	10032	8945
1110	4(1)	0.77(21)	$M1/E2$	$13/2^+ \rightarrow 11/2^+$	9100	7990
1151	3(1)	1.39(25)	$M1/E2$	$7/2^+ \rightarrow 7/2^+$	5925	4775
1153	31(1)	0.76(2)	$M1/E2$	$13/2^+ \rightarrow 11/2^+$	7267	6114
1207	12(3)	1.76(7)	$E2$	$5/2^- \rightarrow 1/2^-$	3848	2640
1259	23(1)	0.80(1)	$M1/E2$	$9/2^+ \rightarrow 7/2^+$	7184	5925
1266	1.5(5)			$(3/2, 11/2) \rightarrow 7/2^-$	10211	8945
1287	6(1)	0.68(9)	$E1$	$3/2^- \rightarrow 1/2^+$	3677	2391
1523	2(1)			$3/2^+ \rightarrow 1/2^+$	3914	2391
1523	2(1)			$11/2^+ \rightarrow 9/2^+$	9209	7686
1579	18(1)	0.84(2)	$E1$	$9/2^- \rightarrow 7/2^+$	6353	4775
1636	≡1000		$M1/E2$	$7/2^+ \rightarrow 5/2^+$	2076	440
1701	0.9(3)			$9/2^+ \rightarrow 7/2^+$	8318	6617
1708	9(1)	0.71(9)	$M1/E2$	$13/2^+ \rightarrow 11/2^+$	9100	7392
1734	13(1)	1.39(12)	$M1/E2$	$13/2^+ \rightarrow 11/2^+$	7267	5533
1756	7(1)	1.15(12)	$M1/E2$	$11/2^+ \rightarrow 13/2^+$	7990	6234
1771	5(2)			$15/2^+ \rightarrow 13/2^+$	9038	7267
1772	180(2)	1.00(1)	$E1$	$5/2^- \rightarrow 7/2^+$	3848	2076
1817	1.3(1)			$11/2^+ \rightarrow 11/2^+$	9209	7392
1821	16(1)	0.83(11)	$E1$	$7/2^- \rightarrow 9/2^+$	8945	7125
1838	4(1)	0.56(8)	$M1/E2$	$5/2^+ \rightarrow 7/2^+$	3914	2076
1859	6(1)	1.20(9)		$11/2^+ \rightarrow 11/2^+$	7392	5533
1943	3(1)			$11/2^+ \rightarrow 13/2^+$	9209	7267
1951	13(1)			$1/2^+ \rightarrow 5/2^+$	2391	440
2010	6(1)	0.91(5)	$M1$	$7/2^+ \rightarrow 5/2^+$	5925	3914
2025	51(3)	1.01(4)	$M1/E2$	$11/2^+ \rightarrow 9/2^+$	9209	7184
2034	8(2)	0.85(7)	$M1/E2$	$17/2^+ \rightarrow 15/2^+$	11072	9038
2072	21(2)			$7/2^+ \rightarrow 9/2^+$	4775	2703
2076	118(8)	1.72(4)	$E2$	$7/2^+ \rightarrow 3/2^+$	2076	0
2194	29(1)	0.67(3)	$M1/E2$	$7/2^- \rightarrow 5/2^-$	6041	3848
2263	589(3)	1.62(6)	$E2$	$9/2^+ \rightarrow 5/2^+$	2703	440
2288	8(2)			$3/2^- \rightarrow 3/2^-$	5965	3678
2325	2(1)			$11/2^- \rightarrow 7/2^-$	11270	8945
2350	4(1)			$9/2^+ \rightarrow 7/2^+$	7125	4775
2362	4(1)			$13/2^- \rightarrow 11/2^+$	10352	7990
2364	38(2)	1.75(15)	$E2$	$7/2^- \rightarrow 3/2^-$	6041	3677
2391	19(2)			$1/2^+ \rightarrow 3/2^+$	2391	0
2441	7(2)			$(13/2^+) \rightarrow 11/2^+$	11650	9209
2457	17(2)	1.82(17)	J^π-J^π	$11/2^+ \rightarrow 11/2^+$	7990	5533
2506	92(1)	1.65(3)	$E2$	$9/2^- \rightarrow 5/2^-$	6353	3848
2535	15(1)	0.64(3)	$M1/E2$	$15/2^+ \rightarrow 13/2^+$	9802	7267
2542	34(1)	0.54(7)	$M1/E2$	$3/2^+ \rightarrow 5/2^+$	2982	440
2592	5(1)			$7/2^- \rightarrow 9/2^-$	8945	6353

TABLE I. *(Continued.)*

E_γ (keV)	I_γ (%)	R_{DCO}	M_λ	Assignment	E_i (keV)	E_f (keV)
2599	4(1)			$13/2^- \rightarrow 11/2^+$	10589	7990
2632	6(1)			$7/2^+ \rightarrow 7/2^+$	9209	6577
2640	31(3)			$1/2^- \rightarrow 3/2^+$	2640	0
2663	4(1)			$9/2^+ \rightarrow 5/2^+$	6577	3914
2674	0.4(1)			$(11/2^+) \rightarrow 7/2^+$	9291	6617
2699	37(2)	1.72(6)	$M1/E2$	$7/2^+ \rightarrow 7/2^+$	4775	2076
2780	14(1)			$9/2^- \rightarrow 7/2^-$	8822	6041
2804	31(2)	0.74(3)	$M1/E2$	$15/2^+ \rightarrow 13/2^+$	9038	6234
2830	142(2)	1.24(2)	$M1/E2$	$11/2^+ \rightarrow 9/2^+$	5533	2703
2866	8(1)	1.63(21)	J^π-J$^\pi$	$13/2^+ \rightarrow 13/2^+$	9100	6234
2911	5(1)			$9/2^+ \rightarrow 7/2^+$	7686	4775
2960	1.1(3)			$13/2^- \rightarrow 11/2^+$	10352	7392
2973	7(1)	1.53(13)	J^π-J^π	$5/2^- \rightarrow 5/2^-$	6819	3847
2982	44(1)			$3/2^+ \rightarrow 3/2^+$	2982	0
2986	9(1)			$13/2^+ \rightarrow 11/2^+$	9100	6114
3095	18(2)	1.82(16)	J^π-J^π	$11/2^+ \rightarrow 11/2^+$	9209	6114
3141	25(2)			$5/2^- \rightarrow 3/2^-$	6819	3677
3237	66(1)			$3/2^- \rightarrow 5/2^+$	3677	440
3274	34(3)	0.60(5)	$M1/E2$	$11/2^- \rightarrow 9/2^-$	9627	6353
3284	7(1)			$11/2^+ \rightarrow 7/2^+$	9209	5925
3322	2(1)			$13/2^- \rightarrow 13/2^+$	10589	7267
3325	7(1)	1.12(11)	$M1/E2$	$3/2^- \rightarrow 1/2^-$	5965	2640
3408	31(2)			$5/2^- \rightarrow 5/2^+$	3848	440
3411	107(1)	1.21(5)	$M1/E2$	$11/2^+ \rightarrow 9/2^+$	6114	2703
3458	39(1)	1.65(7)	$E2$	$11/2^+ \rightarrow 7/2^+$	5533	2076
3474	3(1)			$5/2^+ \rightarrow 5/2^+$	3914	440
3505	5(1)			$15/2^+ \rightarrow 11/2^+$	9038	5533
3531	164(2)	1.82(3)	$E2$	$13/2^+ \rightarrow 9/2^+$	6234	2703
3568	21(1)	1.50(7)	$M1/E2$	$15/2^+ \rightarrow 13/2^+$	9802	6234
3586	24(2)	1.71(17)	$E2$	$11/2^- \rightarrow 7/2^-$	9627	6041
3650	46(1)	1.69(6)	J^π-J^π	$9/2^- \rightarrow 9/2^+$	6353	2703
3811	23(2)			$3/2^- \rightarrow 3/2^-$	7488	3677
3833	16(2)			$(7/2, 11/2) \rightarrow 7/2^-$	9874	6041
3848	69(3)	1.23(5)	$E1/M2$	$5/2^- \rightarrow 3/2^+$	3848	0
3850	18(2)	1.51(6)	$M1/E2$	$7/2^+ \rightarrow 7/2^+$	5925	2076
3874	5(1)			$9/2^+ \rightarrow 9/2^+$	6577	2703
3914	27(3)	1.13(8)	$M1/E2$	$5/2^+ \rightarrow 3/2^+$	3914	0
3920	3(1)	1.10(13)	$M1/E2$	$7/2^+ \rightarrow 5/2^+$	7834	3914
3946	22(2)	1.76(15)	$E2$	$11/2^- \rightarrow 7/2^-$	9987	6041
3999	51(2)	1.61(6)	$E2$	$13/2^- \rightarrow 9/2^-$	10352	6353
4007	6(1)	1.07(8)	$M1/E2$	$(13/2^+) \rightarrow 11/2^+$	9540	5533
4038	32(3)			$11/2^+ \rightarrow 7/2^+$	6114	2076
4047	33(2)	0.83(4)	$M1/E2$	$9/2^- \rightarrow 7/2^+$	8818	4775
4169	13(1)	0.86(11)	$(E1)$	$(11/2^-) \rightarrow 13/2^+$	10403	6234
4177	25(3)	0.86(7)		$(7/2, 11/2) \rightarrow 9/2^+$	6880	2703
4236	5(1)			$13/2^- \rightarrow 9/2^-$	10589	6353
4269	6(1)	1.85(16)	$E2$	$15/2^+ \rightarrow 11/2^+$	9802	5533
4270	2(1)			$15/2^+ \rightarrow 13/2^+$	11537	7267
4278	74(2)	1.01(2)	$E1$	$9/2^- \rightarrow 7/2^+$	6353	2076
4335	75(2)	1.08(2)	$M1$	$7/2^+ \rightarrow 5/2^+$	4775	440
4343	4(1)	0.95(9)	$M1/E2$	$(11/2^-) \rightarrow 9/2^-$	10696	6353
4351	10(2)			$(5/2, 13/2) \rightarrow 9/2^+$	7054	2703
4355	5(1)	1.77(19)	$E1/M2$	$13/2^- \rightarrow 13/2^+$	10589	6234
4422	28(1)	1.51(9)	J^π-J^π	$9/2^+ \rightarrow 9/2^+$	7125	2703
4430	9(1)	0.57(6)	$M1/E2$	$(9/2, 13/2) \rightarrow 11/2^+$	9962	5534
4466	2(1)			$(13/2^+) \rightarrow 11/2^+$	11650	7184
4482	21(2)	1.74(5)	J^π-J^π	$9/2^+ \rightarrow 9/2^+$	7184	2703

TABLE I. *(Continued.)*

E_γ (keV)	I_γ (%)	R_{DCO}	M_λ	Assignment	E_i (keV)	E_f (keV)
4501	20(2)	0.90(4)	$M1/E2$	$9/2^+ \rightarrow 7/2^+$	6577	2076
4524	5(1)			$(9/2, 17/2) \rightarrow 13/2^+$	10758	6234
4564	37(1)	1.50(13)	$E2$	$13/2^+ \rightarrow 9/2^+$	7267	2703
4689	61(1)	1.03(2)	$M1/E2$	$11/2^+ \rightarrow 9/2^+$	7392	2703
4736	4(1)	1.05(9)		$(3/2, 7/2) \rightarrow 5/2^+$	8650	3914
4768	4(1)	0.94(9)	$M1/E2$	$5/2^+ \rightarrow 3/2^+$	7751	2981
4820	6(1)	0.80(5)	$E1$	$13/2^- \rightarrow 11/2^+$	10352	5533
4838	4(1)	1.69(22)	$E2$	$17/2^+ \rightarrow 13/2^+$	11072	6234
4848	3(1)	0.93(9)	$M1/E2$	$3/2^- \rightarrow 1/2^-$	7488	2640
4890	2(1)			$3/2^+ \rightarrow 3/2^+$	7873	2981
4950	1.6(4)			$(3/2, 7/2) \rightarrow 5/2^-$	8797	3848
4983	6(1)	1.11(14)	$M1/E2$	$9/2^+ \rightarrow 9/2^+$	7686	2703
5030	2(1)			$3/2^+ \rightarrow 5/2^+$	8944	3914
5036	6(1)	1.02(7)	$E1$	$11/2^- \rightarrow 13/2^+$	11270	6234
5049	21(1)	0.85(4)	$M1/E2$	$9/2^+ \rightarrow 7/2^+$	7125	2076
5056	12(2)	0.82(3)	$E1$	$13/2^- \rightarrow 11/2^+$	10589	5533
5097	24(1)	1.15(13)	$E1$	$3/2^- \rightarrow 1/2^+$	7486	2391
5108	21(1)	0.98(6)	$M1/E2$	$9/2^+ \rightarrow 7/2^+$	7184	2076
5131	8(2)	1.03(9)	$M1/E2$	$7/2^+ \rightarrow 9/2^+$	7834	2703
5258	10(2)			$(9/2^+) \rightarrow 7/2^+$	10032	4775
5287	42(1)	0.68(2)	$M1/E2$	$11/2^+ \rightarrow 9/2^+$	7990	2703
5292	2(1)	1.00(15)	$E1$	$3/2^- \rightarrow 5/2^+$	9209	3914
5481	9(1)	1.11(18)	$M1/E2$	$3/2^+ \rightarrow 1/2^+$	7873	2391
5484	24(1)	1.54(5)[a]	$M1/E2$	$7/2^+ \rightarrow 5/2^+$	5925	440
5486	2(1)			$(3/2, 7/2) \rightarrow 5/2^+$	9400	3914
5487	3(1)	0.70()		$(5/2, 9/2) \rightarrow 7/2^+$	7563	2076
5615	9(1)	1.63(16)	$E2$	$13/2^+ \rightarrow 9/2^+$	8318	2703
5722	4(1)			$(3/2, 7/2) \rightarrow 3/2^-$	9400	3678
5728	8(1)			$(5/2, 13/2) \rightarrow 9/2^+$	8431	2703
5897	9(2)			$(3/2, 11/2) \rightarrow 7/2^+$	7973	2076
5925	46(3)	1.92(7)	$E2$	$7/2^+ \rightarrow 3/2^+$	5925	0
5990	0.5(1)			$5/2^+ \rightarrow 3/2^+$	8972	2982
6002	3(1)			$(1/2, 9/2) \rightarrow 5/2^+$	9916	3914
6004	2(1)			$15/2^+ \rightarrow 11/2^+$	11537	5533
6114	27(2)	1.65(10)	J^π-J^π	$9/2^- \rightarrow 9/2^+$	8818	2703
6137	20(2)			$9/2^+ \rightarrow 5/2^+$	6577	440
6177	26(2)			$(7/2^+) \rightarrow 5/2^+$	6617	440
6230	1.4(2)	1.53(34)		$(1/2, 5/2) \rightarrow 3/2^+$	9212	2982
6240	24(2)	1.02(5)	$E1$	$7/2^- \rightarrow 9/2^+$	8944	2703
6397	10(2)	1.83(18)	$E2$	$13/2^+ \rightarrow 9/2^+$	9100	2703
6418	0.7(2)			$(1/2, 7/2) \rightarrow 3/2^+$	9400	2982
6436	2(1)			$1/2^+ \rightarrow 1/2^+$	8827	2391
6468	5(1)	1.04(15)		$(7/2, 11/2) \rightarrow 9/2^+$	9171	2703
6553	1.3(2)	1.29(20)	$M1/E2$	$3/2^+ \rightarrow 1/2^+$	8944	2391
6588	14(2)			$(7/2, 11/2) \rightarrow 9/2^+$	9291	2703
6621	18(2)			$(7/2, 11/2) \rightarrow 9/2^+$	9325	2703
6839	19(2)			$(1/2, 9/2) \rightarrow 5/2^+$	7279	440
6872	6(1)			$7/2^- \rightarrow 7/2^+$	8945	2076
6965	21(1)			$(7/2, 9/2)^+ \rightarrow 7/2^+$	9041	2076
7036	33(2)			$(1/2, 9/2) \rightarrow 5/2^+$	7476	440
7171	16(2)	1.09(11)		$(7/2, 11/2) \rightarrow 9/2^+$	9874	2703
7208	22(2)	1.03(5)		$(5/2, 9/2) \rightarrow 7/2^+$	9284	2076
7860	16(1)	0.93(5)	$(E1)$	$(7/2^-) \rightarrow 5/2^+$	8300	440
7993	19(2)	1.08(5)	$(E1)$	$(7/2, 11/2) \rightarrow 9/2^+$	10696	2703
8160	16(2)			$(3/2, 11/2) \rightarrow 7/2^+$	10236	2076
8256	26(2)			$(3/2, 11/2) \rightarrow 7/2^+$	10332	2076
8331	13(2)			$(3/2, 11/2) \rightarrow 7/2^+$	10407	2076

TABLE I. *(Continued.)*

E_γ (keV)	I_γ (%)	R_{DCO}	M_λ	Assignment	E_i (keV)	E_f (keV)
8357	14(1)	0.85(3)	$M1/E2$	$(3/2, 7/2)^+ \rightarrow 5/2^+$	8797	440
8522	2(1)			$(1/2, 9/2) \rightarrow 5/2^+$	8962	440
8601	4(1)			$(7/2, 9/2)^+ \rightarrow 5/2^+$	9041	440
8720	0.5(1)			$(3/2, 11/2) \rightarrow 7/2^+$	10796	2076
8782	1.3(5)			$(3/2, 9/2) \rightarrow 7/2^+$	10859	2076
8845	0.6(1)			$(3/2, 11/2) \rightarrow 7/2^+$	10921	2076
8957	4(1)	0.92(12)	$E1$	$7/2^- \rightarrow 5/2^+$	9397	440
9347	0.4(2)			$(11/2^+) \rightarrow 7/2^+$	11422	2076
9482	4(1)	0.54(9		$(3/2, 7/2) \rightarrow 5/2^+$	9922	440
9594	5(1)	1.01(15)		$(3/2, 7/2) \rightarrow 5/2^+$	10034	440
9714	0.8(2)			$(1/2, 9/2) \rightarrow 5/2^+$	10154	440
9935	2.2(4)			$(3/2, 11/2) \rightarrow 7/2^+$	12011	2076
9996	0.5(1)			$(1/2, 9/2) \rightarrow 5/2^+$	10436	440
10419	0.3(1)			$(3/2, 9/2) \rightarrow 5/2^+$	10859	440

[a]Previously measured $\delta = +4.4(6)$.

excitation energy of 11537 keV, rejecting a $17/2^+$ assignment on the basis of its γ decay to an $11/2^+$ state.

The shell model predicts that the first $17/2^+$ state should appear at 10883 keV with branches of 67% intensity to the lowest $15/2^+$ level at 8871 keV and 32% to the $13/2_2^+$ state at 6214 keV. A candidate for this $17/2^+$ state was located at an excitation energy of 11 072 keV, whose decay branches are in good agreement with the shell- model predictions (Fig. 7). There is, however, a very large discrepancy between the lifetime deduced for this state [50(10) fs], and the shell-model prediction of 3 fs (see Table III). These observations imply a $B(E2)$ strength for the $17/2^+ \rightarrow 13/2^+$ transition of ~ 1 W.u. rather than the shell-model prediction of $B(E2) = 26$ W.u. The contrast with the $15/2^+$ state in the same band is marked since the lifetime extracted for that level is in conformity with the shell-model expectation. The strong deviation for the lowest $17/2^+$ state appears to have the character of a terminating state. Headly *et al.* predict such a $K = 17/2^+$ terminating state in ^{23}Na, within the cranked Nilsson-Strutinksy model, at an excitation energy of 10.6 MeV [52]. Indeed, this is similar to the situation in ^{24}Mg, where the lowest 8^+ level is not a member of the ground-state band or of the excited $K = 2$ band, but rather a spherical configuration or "$d_{5/2}$ condensate".

Note that Thornton *et al.* suggested that the first $17/2^+$ state in ^{23}Na was at 11.29 MeV [30]. No evidence for such a level was found with decay branches to the known high-spin states. A state at 11.27 MeV was located, but the angular correlation analysis and the decay branching indicate that it cannot be a $17/2^+$ state. In fact, an assignment of $11/2^-$ is proposed for this state.

In summary, the yrast line of ^{23}Na was mapped out as far as a terminating configuration with $J^\pi = 17/2^+$. Clearly, the yrast line is less regular and rotational than had been earlier inferred on the basis of transfer reactions. This further illustrates the value of the present γ-ray coincidence measurements in deducing the high-spin structure of these light nuclei.

2. *Excited positive-parity rotational bands*

Earlier studies of the ^{12}C(^{12}C,$p\gamma$) and ^{12}C(^{12}C,$n\gamma$) have focused mainly on the properties of the ground-state band [25,26,28]. Excited bands are more difficult to clearly establish since phase space considerations favor out-of-band branches to the yrast states over low-energy in-band transitions. Nevertheless, in the present work, a large number of high-spin states, particularly in ^{23}Na, were established. The power of coincidence analysis of the γ-γ-γ cubes has allowed several non-yrast rotational bands to be delineated.

In the present work, states have been assigned to the $K = 1/2^+$ band in both ^{23}Na and ^{23}Mg, as far as the $7/2^+$ states at 4775 and 4680 keV, respectively. Thornton *et al.* suggest the 6577-keV state, which is confirmed in this work as $J^\pi = 9/2^+$, as the continuation of the $1/2^+$ band in ^{23}Na [30]. This assignment seems reasonable on the basis of the observed decay to the $5/2^+$ member of the $K = 1/2^+$ band and the associated smooth moment of inertia. It is clear, however, that above 5 MeV it is becoming increasingly difficult either to assign states to rotational bands or to locate clear shell-model counterparts. Indeed, the shell model suggests that this second $9/2^+$ level should be much lower in energy: at 5935 keV in ^{23}Mg and 6033 keV in ^{23}Na. A third $5/2^+$ state is tentatively identified in ^{23}Mg at 5286 keV. The shell model predicts this state at 5196 keV. In ^{23}Na, a plausible analog state would be the known $5/2^+$ level at 5373 keV [44], but its population is not observed in the present work. These observations point to a rather different population of non-yrast states in the two nuclei.

The second $11/2^+$ states in ^{23}Na and ^{23}Mg are identified at 6114 and 5938 keV, respectively, and the second $13/2^+$ levels at 7267 and 7143 keV, respectively. There seems to be no real ambiguity in assigning these as mirror states given their near-identical decay patterns. The mirror energy difference (MED) between these two pairs of levels is, however, somewhat larger than for the other positive-parity states for which the MED is typically small (<50 keV) and negative (see Fig. 9). These

TABLE II. Spectroscopic information for ^{23}Mg from the present work.

E_γ (keV)	I_γ (%)	R_{DCO}	M_λ	Assignment	E_i (keV)	E_f (keV)
178	14(1)			$5/2^- \rightarrow 3/2^-$	3970	3793
450		0.76(1)	$M1/E2$	$5/2^+ \rightarrow 3/2^+$	450	0
663	281(4)	1.12(1)	$M1/E2$	$9/2^+ \rightarrow 7/2^+$	2713	2050
740	20(1)	0.71(4)	$M1/E2$	$13/2^+ \rightarrow 11/2^+$	6192	5452
951	3(1)			$13/2^+ \rightarrow 13/2^+$	7143	6192
956				$5/2^+ \rightarrow 3/2^+$	3859	2903
996	8(2)			$9/2^- \rightarrow 11/2^+$	6448	5452
1023	4(1)			$3/2^- \rightarrow 1/2^-$	3793	2771
1067	3(1)			$5/2^- \rightarrow 3/2^+$	3970	2903
1200	6(1)			$5/2^- \rightarrow 1/2^-$	3970	2771
1207	7(1)			$13/2^+ \rightarrow 9/2^+$	7143	5936
1459	9(1)			$(9/2^+) \rightarrow 7/2^+$	7148	5689
1503	5(1)			$5/2^+ \rightarrow 1/2^+$	3859	2356
1600	≡1000	0.59(1)	$M1/E2$	$7/2^+ \rightarrow 5/2^+$	2050	450
1691	6(1)			$13/2^+ \rightarrow 11/2^+$	7143	5452
1766				$9/2^- \rightarrow 7/2^+$	6446	4680
1808	8(2)			$13/2^+ \rightarrow 11/2^+$	7260	5452
1809	12(2)			$5/2^+ \rightarrow 7/2^+$	3859	2050
1830				$7/2^+ \rightarrow 5/2^+$	5689	3859
1906	62(4)			$1/2^+ \rightarrow 5/2^+$	2356	450
1920	157(5)	0.97(2)	$E1$	$5/2^- \rightarrow 7/2^+$	3970	2050
1967	20(2)	1.34(15)	$M1/E2$	$7/2^+ \rightarrow 9/2^+$	4680	2713
2050	133(11)			$7/2^+ \rightarrow 3/2^+$	2050	0
2158	14(2)	1.28(9)	$M1/E2$	$7/2^- \rightarrow 5/2^-$	6128	3970
2263	665(5)	1.84(1)	$E2$	$9/2^+ \rightarrow 5/2^+$	2713	450
2317	8(1)			$(9/2^-) \rightarrow 11/2^+$	7769	5452
2453	50(2)	1.14(4)	$M1$	$3/2^+ \rightarrow 5/2^+$	2903	450
2478	74(2)	1.73(5)	$E2$	$9/2^- \rightarrow 5/2^-$	6448	3970
2630	55(2)			$7/2^+ \rightarrow 7/2^+$	4680	2050
2739	116(3)	0.49(2)	$M1/E2$	$11/2^+ \rightarrow 9/2^+$	5452	2713
2771	18(1)			$1/2^- \rightarrow 3/2^+$	2771	0
2832	7(2)			$5/2^- \rightarrow 5/2^-$	6802	3970
2903	33(3)			$3/2^+ \rightarrow 3/2^+$	2903	0
3221	4(1)			$3/2^- \rightarrow 1/2^-$	5992	2771
3223	95(3)	0.71(4)	$M1/E2$	$11/2^+ \rightarrow 9/2^+$	5936	2713
3236	27(3)			$5/2^+ \rightarrow 7/2^+$	5286	2050
3343	119(2)	0.99(2)	$E1$	$3/2^- \rightarrow 5/2^+$	3793	450
3402	58(3)	1.80(6)	$E2$	$11/2^+ \rightarrow 7/2^+$	5452	2050
3415	29(6)			$7/2^- \rightarrow 9/2^+$	6128	2713
3480	170(3)	1.89(3)	$E2$	$13/2^+ \rightarrow 9/2^+$	6192	2713
3636	19(2)			$3/2^- \rightarrow 1/2^+$	5992	2356
3735	12(2)			$9/2^- \rightarrow 9/2^+$	6448	2713
3775	31(2)			$(1/2, 5/2) \rightarrow 1/2^+$	6131	2356
3886	18(2)	1.41(12)	$M1/E2$	$11/2^+ \rightarrow 7/2^+$	5936	2050
4188	44(5)	0.62(2)	$M1/E2$	$(9/2^+) \rightarrow 7/2^+$	6238	2050
4230	115(3)	0.59(1)	$M1/E2$	$7/2^+ \rightarrow 5/2^+$	4680	450
4307	24(3)	1.30(18)	J-J	$(9/2^+) \rightarrow 9/2^+$	7020	2713
4325	22(3)	1.62(27)	J-J	$(7/2^+) \rightarrow 7/2^+$	6375	2050
4398	53(2)	0.97(3)	$E1$	$9/2^- \rightarrow 7/2^+$	6448	2050
4418	24(2)			$(1/2, 5/2) \rightarrow 1/2^+$	6774	2356
4430	61(3)[a]			$13/2^+ \rightarrow 9/2^+$	7143	2713
4435	61(3)[a]			$(9/2^+) \rightarrow 9/2^+$	7148	2713
4547	94(2)	0.75(6)	$M1/E2$	$11/2^+ \rightarrow 9/2^+$	7260	2713
4836	25(1)	1.66(8)	J-J	$5/2^+ \rightarrow 5/2^+$	5286	450
4871	5(1)			$(1/2, 5/2) \rightarrow 1/2^+$	7227	2356
4969	16(1)	1.06(4)	$M1/E2$	$(9/2^+) \rightarrow 7/2^+$	7020	2050
5055	11(2)			$(9/2^-) \rightarrow 9/2^+$	7769	2713

TABLE II. *(Continued.)*

E_γ (keV)	I_γ (%)	R_{DCO}	M_λ	Assignment	E_i (keV)	E_f (keV)
5067	8(1)			$11/2^+ \rightarrow 9/2^+$	7780	2713
5240	17(1)	0.44(3)		$(7/2^+) \rightarrow 5/2^+$	5689	450
5300	5(1)			$(5/2, 11/2) \rightarrow 9/2^+$	8015	2713
5399	10(1)	0.98(5)	$M1/E2$	$9/2^+ \rightarrow 7/2^+$	7449	2050
5445	2(1)			$(9/2^+) \rightarrow 7/2^+$	7495	2050
5677	10(1)	0.87(13)	$E1$	$7/2^- \rightarrow 5/2^+$	6128	450
5690	54(4)			$7/2^+ \rightarrow 3/2^+$	5689	0
5729	4(1)	1.42(11)	$E2$	$11/2^+ \rightarrow 7/2^+$	7780	2050
5921	15(1)	2.48(21)	$M1/E2$	$(7/2^+) \rightarrow 5/2^+$	6371	450
5967	2(1)			$(9/2^+) \rightarrow 7/2^+$	8015	2050
6062	32(2)	0.69(3)	$M1/E2$	$(7/2^+) \rightarrow 5/2^+$	6512	450
6110	0.7(1)			$5/2^+ \rightarrow 7/2^+$	8160	2050
6123	7(1)			$(5/2^+) \rightarrow 5/2^+$	6573	450
6353	24(2)			$(7/2^+) \rightarrow 5/2^+$	6803	450
6660	15(1)			$(7/2^+) \rightarrow 5/2^+$	7110	450
6931	28(1)	0.74 (3)	$M1/E2$	$7/2^+ \rightarrow 5/2^+$	7381	450
6998	16(1)	1.58(12)	$E2$	$9/2^+ \rightarrow 5/2^+$	7449	450
7173	5(1)	1.57(24)	$E2$	$9/2^+ \rightarrow 5/2^+$	7623	450
7196	4(1)	0.87(15)	$M1/E2$	$3/2^+ \rightarrow 5/2^+$	7650	450
7334	19(1)	0.89(5)	$M1/E2$	$7/2^{(+)} \rightarrow 5/2^+$	7785	450

[a]Intensity of doublet.

states appear to form a rotational band with the $11/2^+$ state as the bandhead.

The third (and previously known) $7/2^+$ state at 5925 keV in ^{23}Na has been confirmed in the present work and its likely mirror counterpart has been located at 5698 keV in ^{23}Mg. These mirror states share some of the characteristics of the levels discussed above; i.e., the mirror energy difference is rather large (-227 keV). Moreover, there appears to be a strong divergence from the shell-model predictions as the third $7/2^+$ state in ^{23}Na at 5925 keV is not close in energy to the third $7/2^+$ level calculated by the shell model, which is at 5257 keV. For ^{23}Mg, the energy difference is similar: 5698 keV for the experimental $7/2^+$ state compared with 5153 keV in the shell model. These energy differences are rather large given that, for most of the yrast states, the agreement with the shell model to better than 100 keV. It seems likely, however, that the states being compared have the same structure, since the shell model predicts that the transition from the third $7/2^+$ state to the first $5/2^+$ level in ^{23}Na should have a large mixing ratio, $\delta = +4.7$, and the relevant transition (5484 keV) exhibits a strongly mixed dipole character on the basis of its large angular correlation ratio, $R = 1.54(5)$. This also agrees with a previously measured mixing ratio for this transition of $+4.4(6)$ [44]. The same situation pertains to the analogous transition in ^{23}Mg, where the shell model

TABLE III. Lifetimes of selected high-spin states in ^{23}Na and ^{23}Mg; the data are compared with previously measured lifetimes for the mirror states in the analog nucleus, and with the results of an *sd*-shell-model calculation. All lifetimes are in femtoseconds (fs).

Nucleus	E_x (keV)	J^π	τ (fs)	τ_{mirr} (fs)	$E_x^{(sm)}$ (keV)	τ_{sm} (fs)
^{23}Mg	3859	$5/2^+$	12(3)	12(2)	3704	26
	4680	$7/2^+$	10(3)	<2	4616	2
	5286	$5/2^+$	5(2)	0.25(9)	5373	2
	6128	$7/2^-$	18(3)	6.2(14)		
	6192	$13/2^+$	17(3)	22(10)	6138	22
	6448	$(9/2^-)$	35(8)	38(12)		
	7260	$11/2^+$	2(1)		7165	4
^{23}Na	9627	$11/2^-$	4(2)			
	9802	$15/2^+$	4(2)		9567	4
	10352	$13/2^-$	<1			
	11072	$17/2^+$	50(10)		10883	3
	11270	$11/2^-$	18(3)			

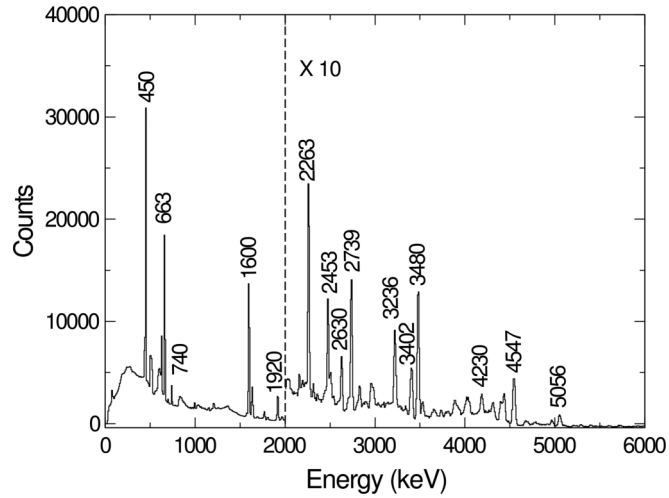

FIG. 3. Sum of double gates on the 450-, 1600-, 663- and 2739-keV transitions in the γ-γ-γ cube. Strong transitions in ^{23}Mg are labeled with their energy in keV.

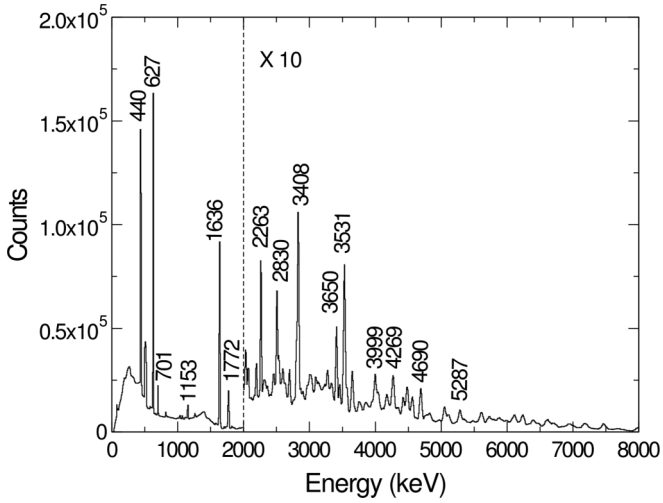

FIG. 4. Sum of double gates on the 440-, 1636-, 627- and 2830- and 701-keV transitions in the γ-γ-γ cube. Strong transitions in ^{23}Na are labeled with their energy in keV.

predicts a very large negative mixing ratio, $\delta = -23.8$, and the measured angular correlation ratio for the transition is markedly low, $R = 0.44(3)$, consistent with a negative mixing ratio. The reasons for the large MED between the respective $7/2^+$ states and the discrepancy with the shell model remain unexplained. The discrepancy does, however, highlight the difficulty of locating shell-model counterparts for the more non-yrast states.

The third $7/2^+$ level at 5925 keV in ^{23}Na appears to be a bandhead state, with a rotational band built on top, which appears to be much more strongly populated in the entry region than the $K = 1/2^+$ band. This rotational sequence comprises the 7184-keV $(9/2^+)$, 9209-keV $(11/2^+)$, and 11650-keV (tentative $13/2^+$) states. The spin and parity of these levels are well constrained both by their decay pattern and by their associated angular correlation ratios. A number of candidate high-spin positive-parity states have been identified in the excitation energy region, 6–10 MeV, in ^{23}Na. The assignment of spin and parity to these levels may be effectively constrained in some instances by decay branchings and angular distributions. On the basis of the angular distribution of the 6177-keV γ ray, $J^\pi = 7/2^+$ is assigned to the state at 6617 keV. This level has very similar properties to the fourth $7/2^+$ state in the shell model at 6477 keV. It is fed via a 1701-keV γ ray from the 8318-keV level, implying a $9/2^+$ assignment to this state. In addition, the states at 6577, 7125, and 7686 keV appear to most likely have $J^\pi = 9/2^+$. Indeed, there is a very plausible shell-model counterpart for the 7125-keV state at 7005 keV.

A number of candidate high-spin states, including two presumed $11/2^+$ states at 7392 and 7990 keV, were located whose shell-model counterparts would be the third and fourth $11/2^+$ levels at 7165 and 7645 keV. There is a likely mirror counterpart for the former at 7260 keV in ^{23}Mg. The state at 9100 keV is proposed as the third $13/2^+$ state, which the shell model predicts to lie at 8468 keV. The spin and parity assignments of these states should be considered as firm on the basis of the decay branchings and angular correlations of the de-exciting γ rays. The general trend indicated by the data is that the experimental positive-parity states are lying somewhat higher than their shell-model counterparts, in some cases up to 700-800 keV. Clearly, this implies that a detailed comparison of high-lying states, particularly of those in the proton-unbound region should be approached with much caution in view of the difference between data and calculations.

C. Negative-parity rotational bands

In the past, negative-parity states in the $A = 23$ nuclei have been discussed within a particle-rotor (PRM) or weak-coupling model (WCM), where these levels arise from the coupling of a single particle or hole to the core [53,54]. In the odd-A = 19–31 nuclei, two $K = 1/2^-$ bands commonly

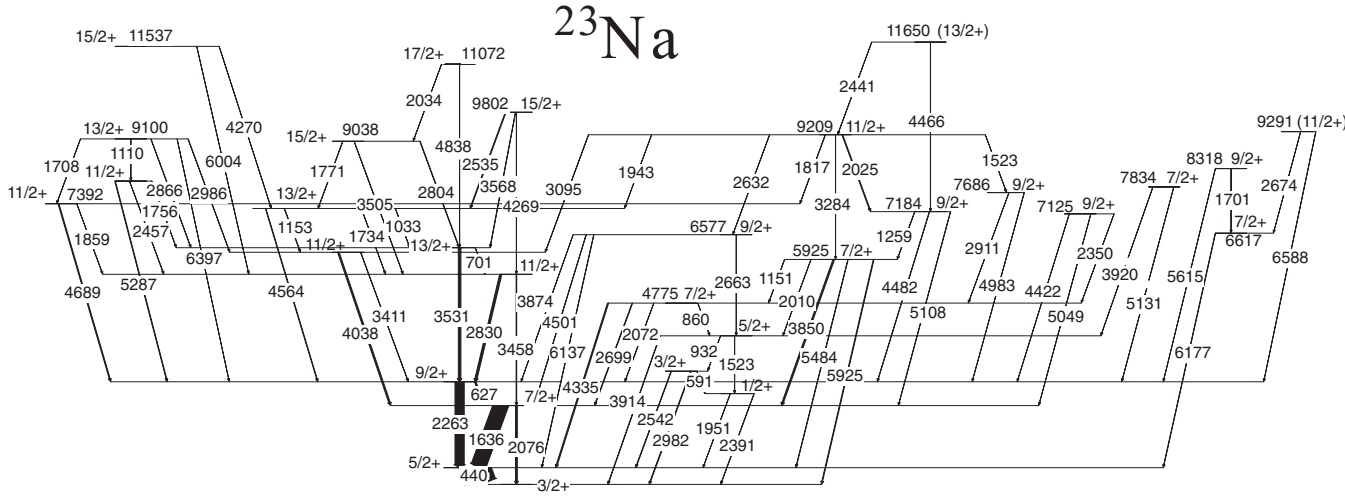

FIG. 5. Positive-parity rotational bands in ^{23}Na. The γ-ray and level energies are given in keV, while the width of the arrows reflects the intensity of the transitions. Many other positive-parity states were identified in the present work, but are suppressed in this figure for reasons of clarity.

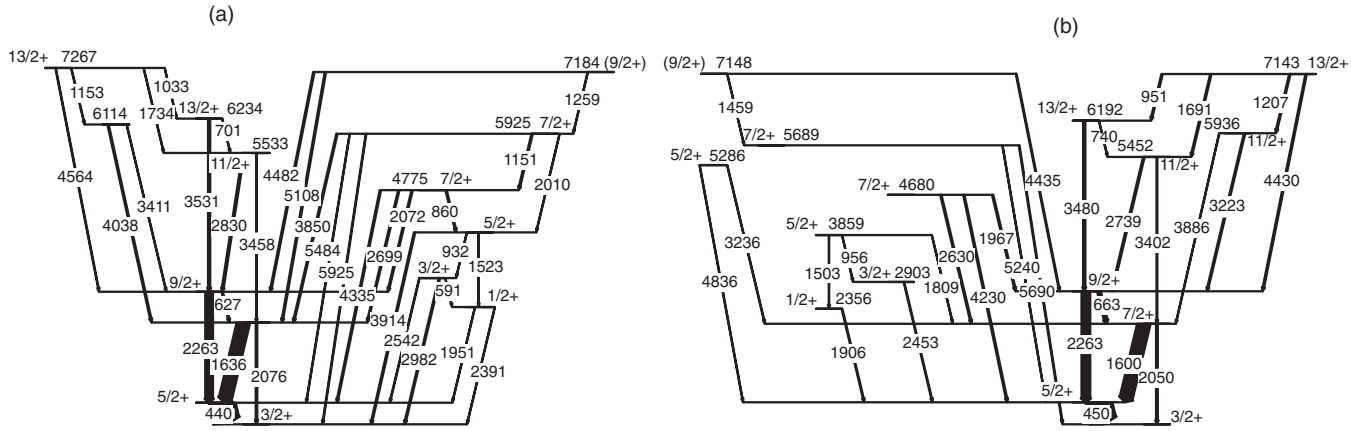

FIG. 6. Comparison of the positive-parity rotational bands in (a) ^{23}Na and (b) ^{23}Mg. The γ-ray and level energies are given in keV, while the width of the arrows reflects the intensity of the transitions. The intensity has been scaled arbitrarily to 100% for the 1600- and 1636-keV transitions in ^{23}Mg and ^{23}Na, respectively.

appear. The first is a hole excitation based on promoting a nucleon from the $1/2^-[101]$ to the $3/2^+[211]$ orbital, and the second is an excited particle band based on the $1/2^-[330]$ Nilsson orbital. In addition, attempts have been made to interpret the negative-parity spectrum in ^{23}Na and ^{23}Mg using a cluster model such as that of Kabir and Buck [55].

In the present work, shell-model calculations were carried out using the PSDPF interaction which describes cross-shell excitations [56]. These largely concur with the particle-rotor description in terms of the origin of the $1/2^-$ to $9/2^-$ states in the first negative-parity band arising from the excitation of a particle from a $p_{1/2}$ orbital into the sd shell. For the $77/2^-$ and $97/2^-$ states, the $p_{3/2}$ contribution is appreciable. For the $117/2^-$ and $13/2^-$ levels, the $f_{7/2}$ component becomes important and mixes with the hole excitation.

1. $K = (1/2^-)_1$ *band*

The $(1/2^-)_1$ band in each nucleus has been delineated as far as the $9/2^-$ and $13/2^-$ states in ^{23}Mg and ^{23}Na, respectively (see Figs. 10 and 11). In addition, lifetimes have been obtained for the first $7/2^-$ and $9/2^-$ states in ^{23}Mg (Table III). The $(1/2^-)_1$ band had previously been identified up to the $9/2^-$ state in ^{23}Na by Frank *et al.* [57], who pointed out that this level decays strongly by an $E1$ transition to the $11/2^+$ state in the ground-state band, which is unexpected on the basis of the normal decay patterns between rotational bands in the Nilsson model. The anomalous strength of this transition was explained in terms of band mixing in the ground-state band which has a configuration primarily involving the $3/2^+[211]$ orbital, but has substantial admixtures of the $1/2^+[211]$, $5/2^+[202]$, and $1/2^+[220]$ states. This conclusion appears to concur with the

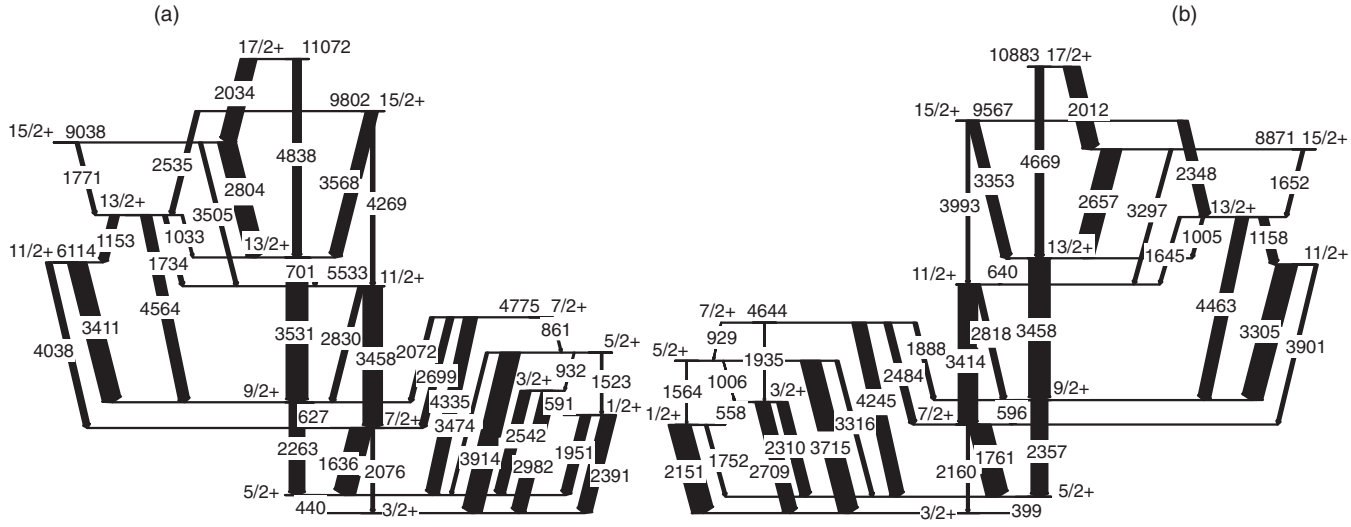

FIG. 7. Comparison of (a) the positive-parity states in ^{23}Na with (b) the predictions of full shell-model calculations described in the text. The decay intensity from each state is normalized to 100% with the width of the arrows corresponding to the fraction of the decay intensity. Weaker transitions are suppressed for the purpose of clarity.

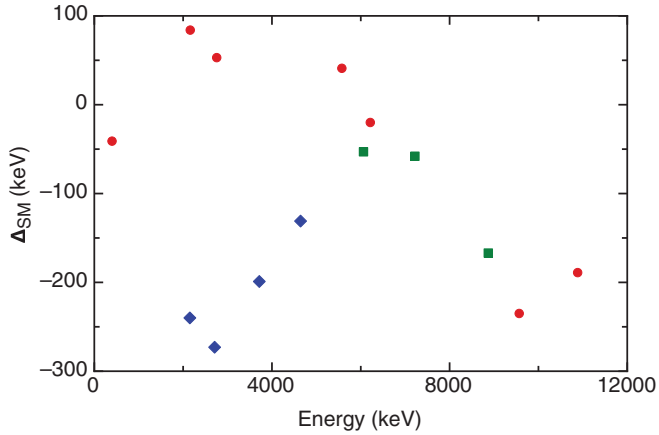

FIG. 8. (Color online) Plot of the difference in excitation energy predicted by the *sd* shell model compared with the experimentally observed states in ^{23}Na. The red circles are for the ground-state band, the blue diamonds are for the excited $K = 1/2^+$ band, and the green squares are for the excited $K = 11/2^+$ band.

results of PSPDF shell-model calculations, which consistently underestimate the strength of $E1$ transitions connecting the negative-parity band to levels in the positive-parity bands. For example, the strongest decay branch from the $5/2^-$ state in ^{23}Na and ^{23}Mg is to the lowest $7/2^+$ level while this branch is essentially zero in the shell-model calculations.

The PSPDF calculations are in excellent agreement for the lowest negative-parity states in ^{23}Na (Fig. 12), but in a manner similar to the USDB-cdpn calculations for positive-parity states, a greater divergence is found as a function of excitation energy. In both cases, the shell model consistently underpredicts the excitation energy of high-lying states with respect to their experimental counterparts.

Experimentally, the MED between the respective states in the lowest negative-parity band is essentially independent of spin and has a magnitude of around +100 keV (Fig. 13). By contrast, the PSPDF calculations predict a near constant MED of around −170 keV. The large discrepancy between theory and experiment could be attributed to the simplicity of the treatment of the MED in the PSPDF calculations, which is only introduced at the level of the $1/r$ dependence in the potential and the Coulomb single-particle energies. Nevertheless, the MEDs predicted by the PSDPF calculations for the positive-parity bands are largely in conformity with those from the standard USDB-cdpn calculations and are in reasonable agreement with data. This may, perhaps, point to the inconsistency regarding MEDs being associated with the intrinsic structure of the negative-parity states being rather more mixed than the calculations imply.

2. *Excited negative-parity structures*

A second negative-parity sequence is observed in both ^{23}Na and ^{23}Mg. The previously known $3/2^-$ and $5/2^-$ members of this structure at 5964 keV and 6819 keV, respectively, in ^{23}Na are confirmed and clear counterparts are found for these states at 5992 and 6802 keV in ^{23}Mg. All of these levels

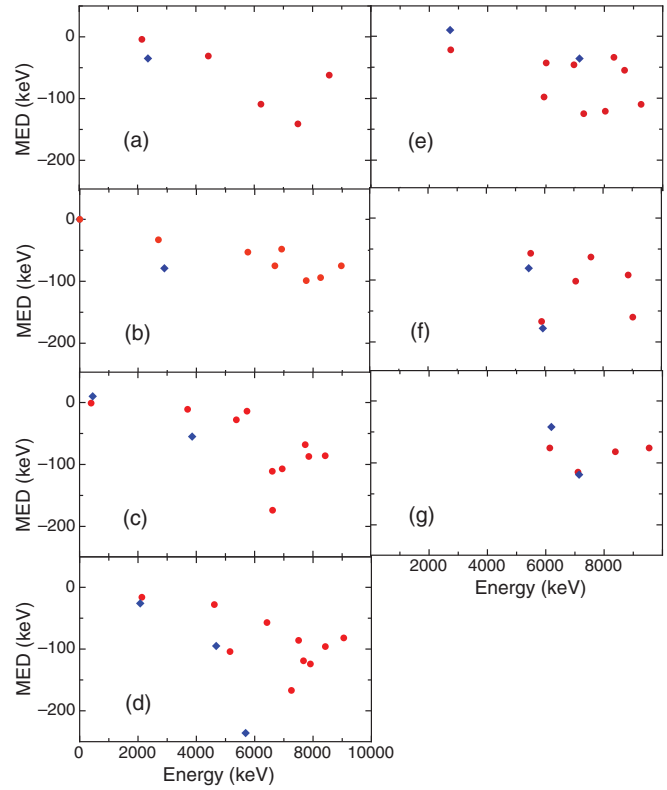

FIG. 9. (Color online) Mirror energy differences (MED) between positive-parity states in ^{23}Na and ^{23}Mg plotted as a function of excitation energy in ^{23}Mg for (a) $J = 1/2$; (b) $J = 3/2$; (c) $J = 5/2$; (d) $J = 7/2$; (e) $J = 9/2$; (f) $J = 11/2$; (g) $J = 13/2$. The blue diamonds are the experimental data, while the red circles are from the *sd*-shell-model calculations described in the text.

decay primarily to states in the first negative-parity band. This implies mirror energy differences of less than 30 keV in both cases (Fig. 13).

It is clearly more difficult to locate excited negative-parity states than positive-parity ones in these nuclei, since no polarization measurements are available which would make it possible to convincingly distinguish between $E1$ and $M1$ transitions. The PSPDF shell-model calculations also predict a large number of states in the higher-energy region of interest for nuclear astrophysics (see Fig. 14). Moreover, as discussed above in the context of the first negative-parity band, $E1$ transitions are sensitive to variations in strength due to band mixing or isospin mixing. The PSPDF calculations struggle to reproduce the observed branching ratios for $E1$ transitions. Accepting these caveats, there are some indications of where high-lying negative-parity states might lie in ^{23}Na from previous reaction studies. Accordingly, a number of such higher-lying negative-parity states (Fig. 11). The existence of a $7/2^-$ level in ^{23}Na at 8945 keV, which was known from previous work, has been confirmed. In a ^{19}F(^{6}Li,d) study, Fortune *et al.* identified a level with $E_x = 8822$ keV and determined that the associated angular momentum transferred was $\ell = 5$ [29]. This would imply spin possibilities of $9/2^-$ or $11/2^-$ for this level. In the present work, the existence of this state is confirmed and its decay to a known $7/2^+$ level

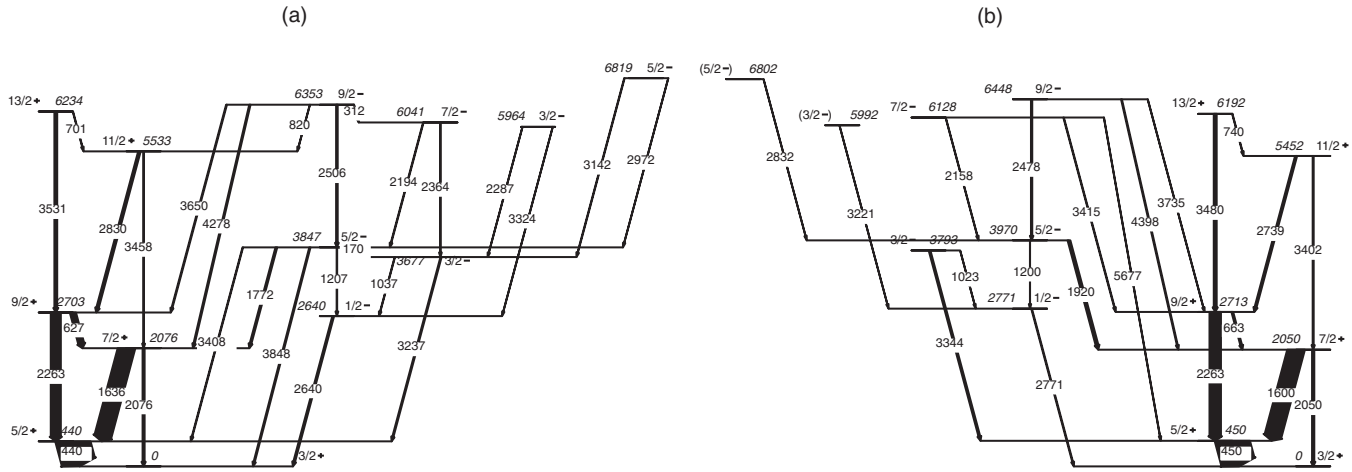

FIG. 10. Comparison of the negative-parity bands in (a) ^{23}Na and (b) ^{23}Mg; level and transition energies are given in keV. The width of the arrows denotes the relative strength of decay branches.

at 4775 keV is established. This observation would favor a $9/2^-$ assignment to the 8822-keV level. A firm candidate for an $11/2^-$ state is at 11720 keV. This level decays both to the well established $7/2^-$ state at 8945 keV as well as to the yrast $13/2^+$ state (by a dipole transition). Such a decay branching allows only an $11/2^-$ assignment. In addition, a second $13/2^-$ state at 10589 keV is tentatively proposed. This state decays weakly to the first $9/2^-$ level, as well as to the yrast $11/2^+$

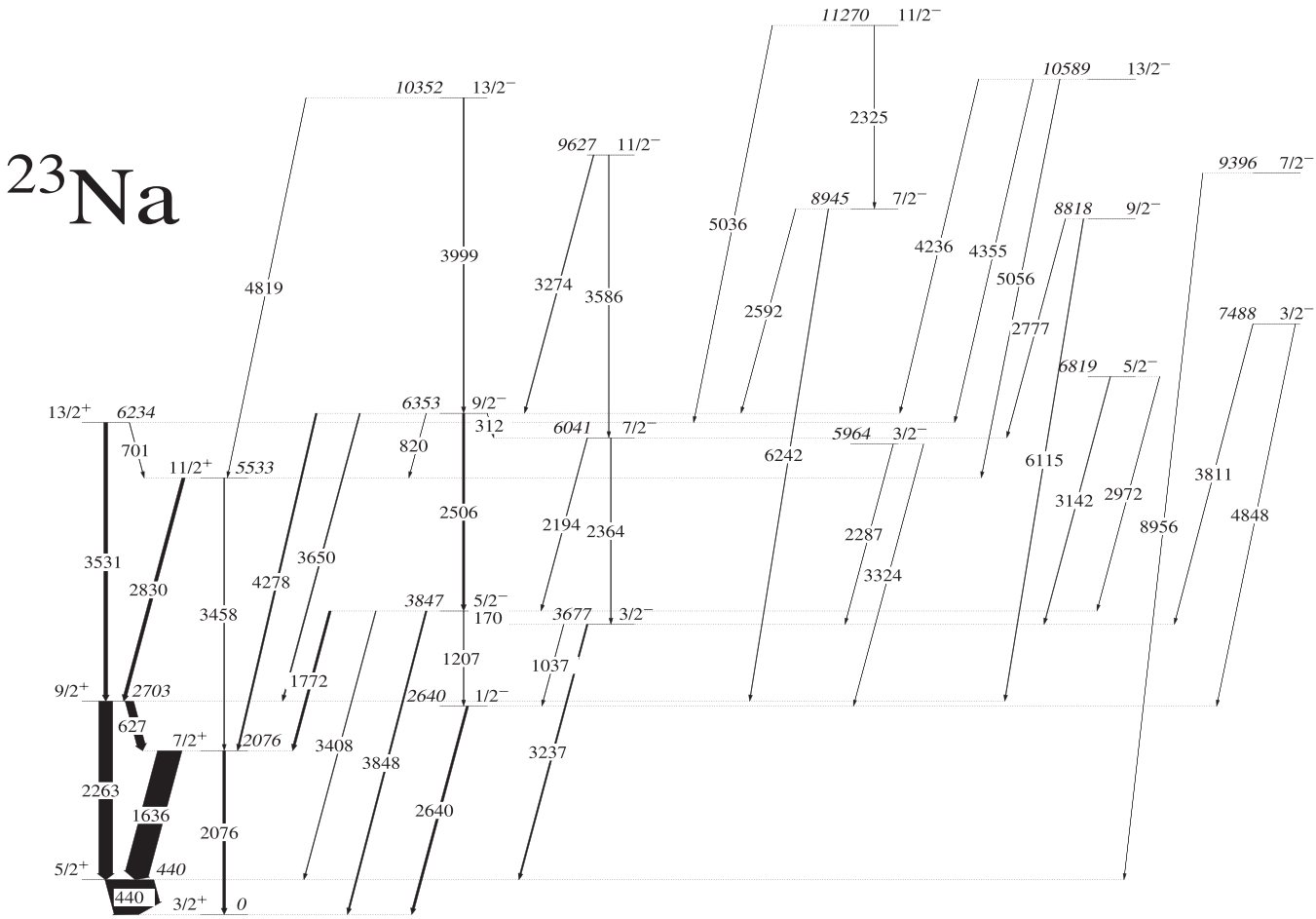

FIG. 11. States of presumed negative parity in ^{23}Na; level and transition energies are given in keV. The width of the arrows denotes the relative strength of the decay branches.

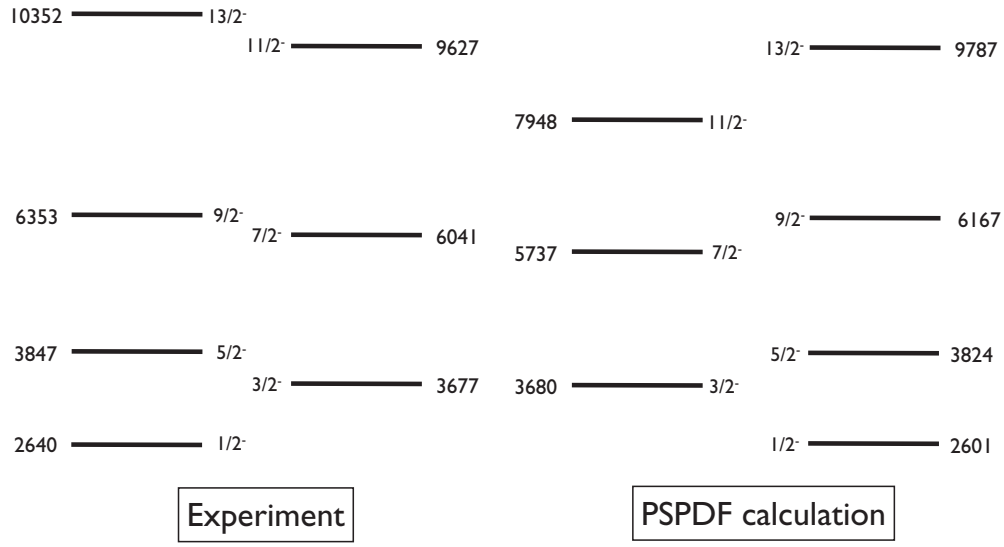

FIG. 12. Comparison of the yrast negative-parity states in ^{23}Na [the K $= (1/2^-)_1$ band] with the predictions of the PSPDF shell model (not to scale).

state via a stretched-dipole transition and to the $13/2^+$ state with a transition consistent with it being of unstretched-dipole ($E1$) character.

VI. PROTON-UNBOUND STATES OF ASTROPHYSICAL INTEREST

A. States of relevance to the ^{22}Na(p,γ) reaction: Proton unbound states in ^{23}Mg

In this section, the properties of unbound states in ^{23}Mg are discussed. Portions of the relevant data have already been published [12] and some of the preliminary conclusions are superseded by more direct measurements.

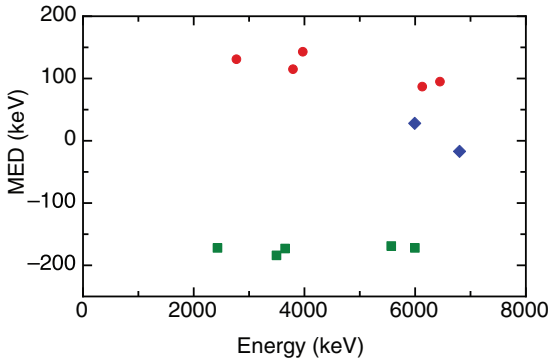

FIG. 13. (Color online) Mirror energy differences (MED) between negative-parity states in ^{23}Na and ^{23}Mg plotted as a function of excitation energy in ^{23}Mg. The red circles are for the $K = (1/2^-)_1$ band, while the blue diamonds are for the second negative-parity band. The green squares are calculated values for the MED for the first negative-parity band, obtained using PSPDF shell-model calculations (see text).

1. Near-threshold states: E_x = 7623 and 7647 keV

These levels are too close to the proton-threshold to be a target for direct studies [40] and indirect techniques are therefore essential. Firm spin assignments for the previously reported 7623- and 7647-keV levels have now been made. In an earlier ^{24}Mg(p, d) study, the angular distribution of the particle groups corresponding to the 7623-keV state were assigned a multipolarity $L = 4$; i.e., the available spin possibilities are $7/2^+$ and $9/2^+$ [35]. The 7173-keV γ ray which depopulates the 7623-keV state has an angular correlation ratio consistent with an $E2$ assignment. Since it feeds a known $5/2^+$ level, the $7/2^+$ possibility is ruled out and a spin-parity of $9/2^+$ can be confidently assigned to the 7623-keV level. Similar arguments firmly fix the 7647-keV level as $J^\pi = 3/2^+$. A possible mirror counterpart for the 7647-keV state is the state at 7873 keV in ^{23}Na. These states both exhibit decay branches to the first $5/2^+$ and $1/2^+$ levels. The 7873-keV state in ^{23}Na has been previously assigned spin possibilities of $3/2^+$ or $5/2^+$ [44]. Since, this state is seen in the present work and it decays to the $1/2^+$ state at 2391 keV by a dipole transition, a $J^\pi = 3/2^+$

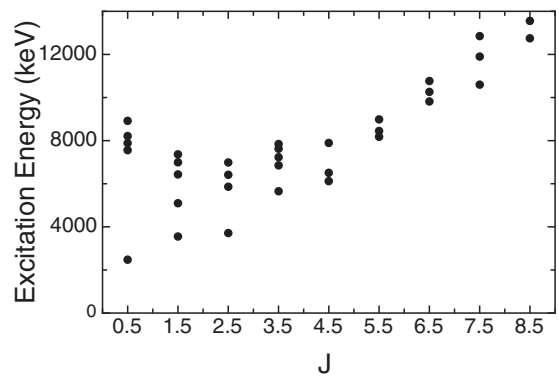

FIG. 14. PSPDF calculations of negative-parity states in ^{23}Na.

assignment is proposed. If these were indeed mirror states, then it would imply a MED of -225 keV, broadly consistent with the observed trend for positive-parity states (Fig. 9).

It is somewhat more difficult to find a mirror counterpart for the 7623-keV state in ^{23}Mg. In all discussion of mirror assignments, it should be remarked that it is entirely possible that further decay branches have been missed. For example, it is not possible to observe ground-state transitions, as the triggering conditions require at least two coincident γ rays. Moreover, some of the coincident gates do not yield sufficiently clean spectra to allow an unambiguous assignment of the transitions. On first inspection, two possible candidates for mirror states would appear to be the 7751- or 7834-keV states in ^{23}Na. Coincidence measurements and angular distributions from the present work clearly indicated that these two levels have $J^\pi = 5/2^+$ and $7/2^+$, respectively. They would not, therefore, seem to be good mirror partners given that $J^\pi = 9/2^+$ is assigned to the ^{23}Mg state at 7623 keV, and, in any case, the decay branchings are very different.

A theoretical study by Comisel *et al.* [58] broadly supports the above conclusions regarding the threshold states, through a study of the mirror symmetry of states in ^{23}Na and ^{23}Mg via calculations of MEDs and Thomas-Ehrman shifts.

2. *States at E_x = 7769, 7780, and 7783 keV*

The state at 7783 keV, previously reported by Stegmüller *et al.* [34], is confirmed and also observed to decay solely to the 450-keV, $5/2^+$ level by a dipole transition. The updated excitation energy for this level is 7785 keV and its proposed spin-parity is $7/2^{(+)}$. It is again difficult to locate a mirror partner for this level. Indeed, the $7/2^+$ state at 7834 keV in ^{23}Na has very different branching as discussed above.

Two new states were identified in this energy region, however. A level at 7769 keV was observed which decays to both the lowest $9/2^+$ and $11/2^+$ states [12], in addition to a previously unreported state at 7780 keV, which decays to the $7/2^+$ and $9/2^+$ states in the yrast band. This sensitivity to additional levels is one of the key advantages of the present approach as compared to transfer reaction studies with their more limited resolution.

B. States of relevance to the ^{22}Ne(p,γ) reaction: Proton unbound states in ^{23}Na

The situation concerning levels in ^{23}Na is a little less favorable for the present methodology than for ^{23}Mg because they lie at higher excitation energy. Moreover, ^{22}Ne has a ground-state spin-parity of 0^+ rather than the 3^+ value of ^{22}Na, so the states of most relevance in the compound system are of low rather than high spin. In the present work, a large number of states were identified in the proton-unbound region in ^{23}Na. In addition to decays to the yrast band, many branches to non-yrast states such as the first $1/2^-$, $1/2^+$, and $3/2^+$ levels were found. The characteristics of proton-unbound states in ^{23}Na are reviewed below and compared with the existing literature for states up to 9.2 MeV. Some additional states above this energy are observed and reported in Table I.

1. *E_x = 8797 keV*

Two γ rays deexcite this previously known, near-threshold level. The decay branching and angular distribution of the 8357-keV γ ray favors a spin assignment of 3/2 or 7/2 to the 8797-keV state. In any event, the energy of this level is so close to threshold, that its impact on the astrophysical reaction rate is negligible.

2. *E_x = 8818 keV*

As discussed in the earlier section on negative-parity states, this level can be associated with the 8822(3) keV level identified in a ^{19}F(^{6}Li,d) study by Fortune *et al.* [29]. The observed angular distributions and γ-ray branchings, when combined with the $\ell = 5$ transfer observed by Fortune *et al.*, would fix the spin-parity of this state at $9/2^-$. Clearly, the high angular momentum transfer means that the contribution of this state to the total reaction rate would be very small.

3. *E_x = 8827 keV*

Several measurements are reported in the literature for this $1/2^+$ state. The first comes from a ^{22}Ne(d, n) study by Christiansson *et al.* [59]. Görres *et al.* obtained an energy for this state of 8829.5(7) keV in their ^{22}Ne(p,γ) measurement [60]. Later, ^{23}Na(γ,γ') data by Vodhanel *et al.* [61] reported a somewhat different level energy of 8826(2) keV. Clearly, these values differ by more than one standard deviation. Moreover, in the present work, a level energy of 8826.5(19) keV is obtained which would be more consistent with the latter literature value. The recent reevaluation of the ^{22}Ne(p,γ) reaction rate by Hale *et al.* employed the more precise level energy derived by Görres *et al.* [60], in preference to their own measured value of 8830(3) keV [42]. The peak which they observe in the deuteron spectrum, however, sits on the side of a very large resonance associated with proton transfer on a ^{16}O contaminant (to the first excited state in ^{17}F). The value obtained in this transfer work [8830(3) keV] would be compatible with all the other values discussed above. In deriving reaction rates in the future, employing a weighted average of recent measurements for this level energy seems appropriate.

4. *E_x = 8862, 8894, and 9000 keV*

Powers *et al.* report tentative states with excitation energies of 8862, 8894, and 9000 keV from a (^{3}He,d) reaction [62]. However, these states have not been observed in any other reaction study conducted since [41,42] nor is there any evidence for these in the present measurement—if these states do exist their γ decay must be correspondingly weak.

5. *Doublet of states with E_x = 8945 keV*

The present analysis provides compelling evidence for the existence of two states at an excitation energy of 8944 keV, rather than the single one reported by both Görres *et al.* [41] and Hale *et al.* [42]. These two states can be distinguished

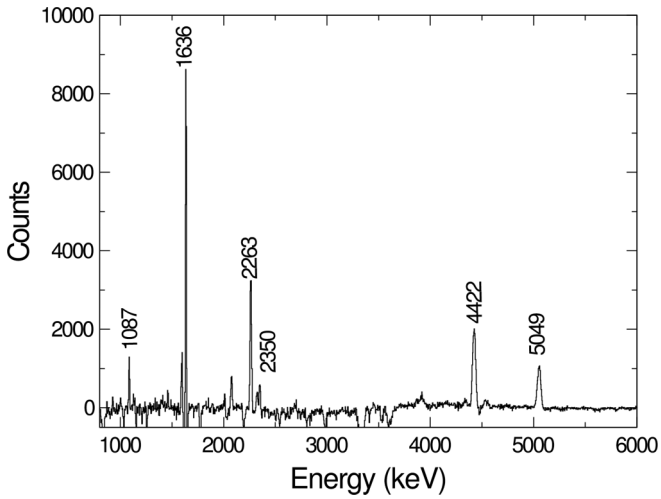

FIG. 15. Spectrum gated by the 1821-keV γ ray, which depopulates the $7/2^-$ state at 8945 keV. The 1087-keV γ ray feeding this level is clearly visible as are the transitions below the 1821-keV γ ray in the decay scheme.

since one of them is fed by a 1087-keV γ ray while the other is not, see Fig. 15. Gating on this γ ray, coincident transitions are found indicating decay branches from this first 8944 keV state, which are consistent with a spin-parity of $J^\pi = 7/2^-$ for that state, since it decays to a $9/2^+$ and $5/2^+$ level by dipole transitions. Coincidence relationships firmly establish the presence of a second lower-spin state at 8944 keV which is not fed by the 1087-keV line (see Fig. 16). On the basis of its decay branches and angular correlation ratios, this second state is tentatively assigned a spin-parity of $3/2^+$.

The first of these two 8944-keV states, which decays to the $9/2^+$ state at 2704 keV, is clearly the same as the previously known state at 8945 keV on the basis of its decay branches. The present J^π assignment of $7/2^-$ is consistent with the reported $\ell = 3$ transfer from a (d, n) study [63]. However,

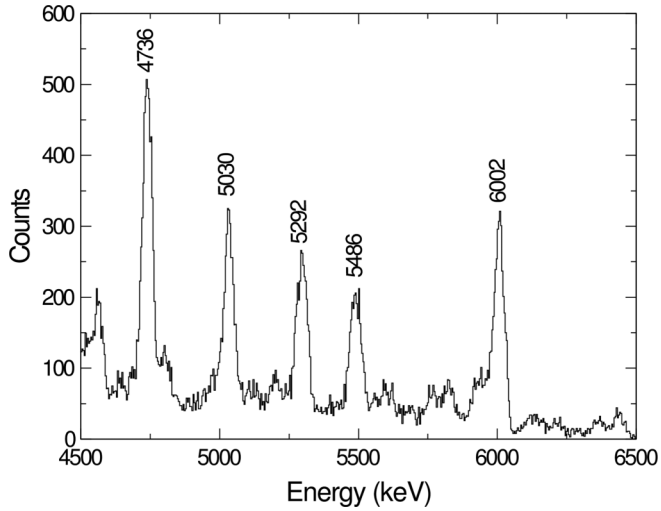

FIG. 16. Spectrum gated by the 3914-keV γ ray, which depopulates the $5/2^+$ state at 3914 keV. The 5030- and 5292-keV γ rays which depopulate the astrophysically relevant states at 8944 and 9211 keV in ^{23}Na, are marked.

Childs *et al.* report a strong compound nuclear contribution to the cross section which leads them to caution on the reliability of this angular momentum assignment [63]. Moreover, Powers *et al.* report an angular distribution for this state inconsistent with a pure, first-order direct process [62]. Hale *et al.* cannot distinguish between $\ell = 2$ or $\ell = 3$ transfer for this level. Most likely, it is the presence of these two near-degenerate states at 8944 keV that leads to these ambiguous angular distributions and demonstrates the advantage of the present analysis in resolving these ambiguities. Given the observed level density of $\sim$3 levels per 100 keV at the energies above the proton threshold in ^{23}Na, the accidental overlap of two such levels is clearly a non-negligible possibility.

6. $E_x = 8972$ keV

Hale *et al.* find that the 8972-keV state may be associated with transfer of either a $d_{5/2}$ or $f_{7/2}$ proton [42]. In the present work, this state is found to decay only to a $3/2^+$ level. Since an $M2$ transition may be ruled out on lifetime grounds, the possibility of a $7/2^-$ assignment may be rejected and this state, therefore, most likely has spin-parity $5/2^+$.

7. Doublet of $E_x = 9038$ and 9041 keV

It is remarkable that there is a second doublet of states above the proton threshold. In common with the doublet at 8945 keV, the two states at 9038 and 9041 keV are clearly resolvable, not only on the basis of their slightly different excitation energies, but also from the fact that one of the levels is of high spin, $J^\pi = 15/2^+$, and is fed by a 2034-keV γ ray from a $17/2^+$ state. It seems clear that Hale *et al.* have confused this high-spin state with the second level which has decay branches to a $5/2^+$ and $7/2^+$ state [42], and is completely consistent with a spin-parity of $7/2^+$ or $9/2^+$, as suggested by the angular distribution measurement of Görres *et al.* [41]. The latter data are consistent with a $g_{7/2}$ transfer.

8. $E_x = 9103$ keV

No evidence was found for a previously observed state at 9072 keV, while for the previously known state at 9103 keV, an updated energy of 9100 keV was determined together with the assignment of a spin-parity of $13/2^+$, which is well supported by both decay branchings, angular distributions and the relative population of this level. The next reported states at 9113 and 9147 keV are not observed in this work.

9. $E_x = 9171$ keV

A γ decay from this state to a $9/2^+$ level is observed with an associated dipole multipolarity implying a relatively high-spin for this state.

VII. CONCLUSION

The γ decay of a large number of excited states in the mirror nuclei, ^{23}Na and ^{23}Mg was investigated making use of the ^{12}C(^{12}C,p) and ^{12}C(^{12}C,n) reactions, respectively.

Extensive decay schemes have been produced for states of inferred positive and negative parity. For ^{23}Na, the details of the high-spin structure have been clarified, and a candidate terminating state with $J^{\pi} = 17/2^{+}$ has been identified. MEDs have been examined for both positive and negative parity states. USDB-cdpn calculations appear to give a reasonable reproduction of experimentally observed MEDs and could be used to provide reasonable predictions of the location of unobserved mirror states which might be of interest in nuclear astrophysics-related applications. For the negative-parity states, MEDs may be extracted, but the present PSPDF shell model struggles to reproduce them. Moreover, it also has difficulty in reproducing the observed $E1$ transitions connecting the respective rotational bands. The present understanding of negative-parity states is, therefore, of more limited utility, and it is here that additional theoretical work would be of benefit if robust predictions about mirror states are to be made. In addition to the discussion of nuclear structure issues, this paper addresses the impact of the present work so far as the details of states in the Gamow window for the astrophysical interesting ^{22}Na$(p,\gamma)^{23}$Mg and ^{22}Ne$(p,\gamma)^{23}$Na reactions are concerned.

ACKNOWLEDGMENTS

Discussions with Gavin Lotay, Mike Bentley, John Wood, Oliver Kirsebom and Antti Saistamoinen are gratefully acknowledged. This work was supported in part by the US Department of Energy, Office of Nuclear Physics, under Contract No. DE-AC02-06CH11357.

[1] M. A. Bentley and S. Lenzi, Prog. Part. Nucl. Phys. **59**, 497 (2007).
[2] D. D. Warner, M. A. Bentley, and P. van Isacker, Nat. Phys. **2**, 311 (2006).
[3] M. A. Bentley, C. D. O'Leary, G. Martinez-Pinedo, D. E. Appelbe, R. A. Bark, D. M. Cullen, S. Ertürk, and A. Maj, Phys. Lett. B **437**, 243 (1998).
[4] C. D. O'Leary *et al.*, Phys. Rev. Lett. **79**, 4349 (1997).
[5] J. Ekman *et al.*, Phys. Rev. Lett. **92**, 132502 (2004).
[6] D. G. Jenkins *et al.*, Phys. Rev. C **72**, 031303 (2005).
[7] N. S. Pattabiraman *et al.*, Phys. Rev. C **78**, 024301 (2008).
[8] J. José, M. Hernanz, and C. Iliadis, Nucl. Phys. A **777**, 550 (2006).
[9] J. Casanova, J. José, E. Garciá-Berro, S. N. Shore, and A. C. Calder, Nature (London) **478**, 490 (2011).
[10] S. Bishop *et al.*, Phys. Rev. Lett. **90**, 162501 (2003).
[11] I. Y. Lee, Nucl. Phys. A **520**, 641c (1990).
[12] D. G. Jenkins *et al.*, Phys. Rev. Lett. **92**, 031101 (2004).
[13] D. Seweryniak *et al.*, Phys. Rev. Lett. **94**, 032501 (2005).
[14] D. Seweryniak *et al.*, Phys. Rev. C **75**, 062801 (2007).
[15] D. G. Jenkins *et al.*, Phys. Rev. C **73**, 065802 (2006).
[16] G. Lotay *et al.*, Phys. Rev. C **77**, 042802 (2008).
[17] G. Lotay, P. J. Woods, D. Seweryniak, M. P. Carpenter, R. V. F. Janssens, and S. Zhu, Phys. Rev. C **80**, 055802 (2009).
[18] G. Lotay, P. J. Woods, D. Seweryniak, M. P. Carpenter, H. M. David, R. V. F. Janssens, and S. Zhu, Phys. Rev. C **84**, 035802 (2011).
[19] A. E. Champagne *et al.*, Nucl. Phys. A **556**, 123 (1993).
[20] D. G. Jenkins *et al.*, Phys. Rev. C **86**, 064308 (2012).
[21] I. Wiedenhöver *et al.*, Phys. Rev. Lett. **87**, 142502 (2001).
[22] Y. Fujita *et al.*, Phys. Rev. Lett. **92**, 062502 (2004).
[23] C. A. Grossmann, M. A. LaBonte, G. E. Mitchell, J. D. Shriner, J. F. Shriner, G. A. Vavrina, and P. M. Wallace, Phys. Rev. C **62**, 024323 (2000).
[24] J. F. Shriner, G. E. Mitchell, and B. A. Brown, Phys. Lett. B **586**, 232 (2004).
[25] D. Evers, G. Denhöfer, W. Assmann, A. Harrasim, P. Konrad, C. Ley, K. Rudolph, and P. Sperr, Z. Phys. A **280**, 287 (1977).
[26] G. J. Kekelis, A. H. Lumpkin, and J. D. Fox, Phys. Rev. Lett. **11**, 710 (1975).
[27] G. J. Kekelis, A. H. Lumpkin, K. W. Kemper, and J. D. Fox, Phys. Rev. C **15**, 664 (1977).
[28] H. T. Fortune and K. Wells, Phys. Rev. C **30**, 527 (1984).
[29] H. T. Fortune, J. R. Powers, and L. Bargeron, Phys. Rev. C **51**, 1154 (1995).
[30] S. T. Thornton, D. E. Gustafson, K. R. Cordell, L. C. Dennis, T. C. Schweizer, and J. L. C. Ford, Phys. Rev. C **17**, 576 (1978).
[31] D. E. Gustafson, S. T. Thornton, T. C. Schweizer, J. L. C. Ford, P. D. Miller, R. L. Robinson, and P. H. Stelson, Phys. Rev. C **13**, 691 (1976).
[32] Y. Fujita *et al.*, Phys. Rev. C **66**, 044313 (2002).
[33] S. Seuthe *et al.*, Nucl. Phys. A **514**, 471 (1990).
[34] F. Stegmüller, C. Rolfs, S. Schmidt, W. H. Schulte, H. P. Trautvetter, and R. W. Kavanagh, Nucl. Phys. A **601**, 168 (1990).
[35] S. Kubono *et al.*, Z. Phys. A **348**, 59 (1994).
[36] S. Schmidt, C. Rolfs, W. H. Schulte. H. P. Trautvetter, R. W. Kavanagh, C. Hategan, S. Faber, B. D. Valnion, and G. Graw, Nucl. Phys. A **591**, 227 (1995).
[37] V. E. Iacob *et al.*, Phys. Rev. C **74**, 045810 (2006).
[38] A. Saastamoinen *et al.*, Phys. Rev. C **83**, 045808 (2011).
[39] O. S. Kirsebom *et al.*, Eur. Phys. J. A **47**, 130 (2011).
[40] A. L. Sallaska, C. Wrede *et al.*, Phys. Rev. C **83**, 034611 (2011); A. L. Sallaska, C. Wrede, A. Garcia, D. W. Storm, T. A. D. Brown, C. Ruiz, K. A. Snover, D. F. Ottewell, L. Buchmann, C. Vockenhuber, D. A. Hutcheon, and J. A. Caggiano, Phys. Rev. Lett. **105**, 152501 (2010).
[41] J. Görres *et al.*, Nucl. Phys. A **385**, 57 (1982).
[42] S. E. Hale, A. E. Champagne, C. Iliadis, V. Y. Hansper, D. C. Powell, and J. C. Blackmon, Phys. Rev. C **65**, 015801 (2001).
[43] B. M. Nyako *et al.*, Phys. Rev. Lett. **52**, 507 (1984).
[44] *Table of Isotopes*, Vol. 1, edited by R. B. Firestone and V. S. Shirley (John Wiley & Sons, New York, 1996).
[45] E. Ormand and B. A. Brown, Nucl. Phys. A **491**, 1 (1989).
[46] B. A. Brown and W. A. Richter, Phys. Rev. C **74**, 034315 (2006).
[47] http://www.nscl.msu.edu/~brown/resources/resources.html.
[48] W. A. Richter, S. Mkhize, and B. A. Brown, Phys. Rev. C **78**, 064302 (2008).
[49] P. W. Green *et al.*, Phys. Rev. C **12**, 887 (1975).
[50] B. B. Back *et al.*, Phys. Rev. C **13**, 875 (1976).
[51] G. D. Jones *et al.*, Phys. Rev. C **12**, 132 (1975).
[52] D. M. Headly, R. K. Sheline, and I. Ragnarsson, Phys. Rev. C **49**, 222 (1994).
[53] M. Guttormsen, T. Pedersen, J. Rekstad, T. Engeland, E. Sones, and F. Ingebretsen, Nucl. Phys. A **338**, 141 (1980).

[54] T. Pedersen, E. Osnes, and M. Guttormsen, Nucl. Phys. A **332**, 1 (1979).
[55] A. Kabir and B. Buck, Nucl. Phys. A **518**, 449 (1990).
[56] M. Bouhelal *et al.*, Nucl. Phys. A **864**, 113 (2011).
[57] G. G. Frank, M. W. Greene, D. T. Kelly, A. A. Pilt, and J. A. Kuehner, Phys. Rev. Lett. **28**, 571 (1972).
[58] H. Comisel, C. Hategan, G. Graw, and H. H. Wolter, Phys. Rev. C **75**, 045807 (2007).
[59] J. E. Christiansson, J. Dubois, H. Odelius, and H. Roth, Phys. Scr. **10**, 65 (1975).
[60] J. Görres *et al.*, Nucl. Phys. A **408**, 372 (1983).
[61] R. Vodhanel, M. K. Brussel, R. Moreh, W. C. Sellyey, and T. E. Chapuran, Phys. Rev. C **29**, 409 (1984).
[62] J. R. Powers, H. T. Fortune, R. Middleton, and O. Hansen, Phys. Rev. C **4**, 2030 (1971).
[63] W. A. Childs, R. C. Ritter, B. D. Murphy, and R. M. Strang, Nucl. Phys. A **203**, 133 (1973).